2026
Advancing Coral Reef Research and Resilience in Southeast Florida: Phase 6

Final Report

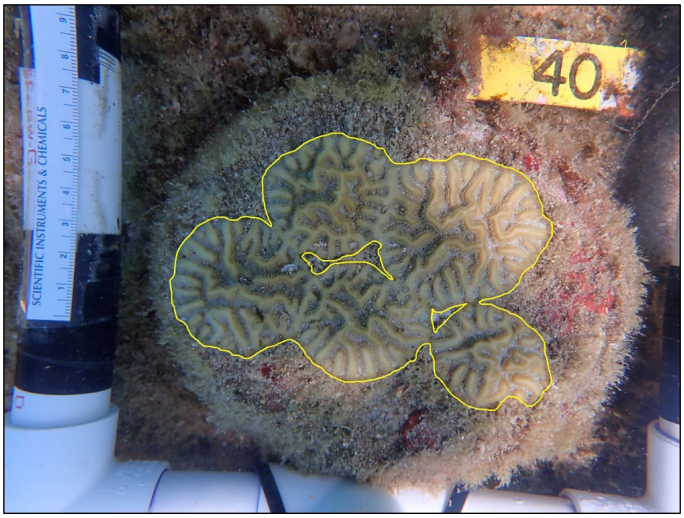

Advancing Coral Reef Research and Resilience in Southeast Florida: Phase 6

Final Report

Prepared by:
Joshua D. Voss, Olivia Faris, Gabrielle Pantoni, Ryan Eckert, Haley Davis, and Milena Nesic

Florida Atlantic University
Harbor Branch Oceanographic Institute
5600 US Highway 1 North
Fort Pierce, FL 34946

June 15, 2026

Completed in fulfillment of C5F346 for

Florida Department of Environmental Protection
Coral Protection and Restoration Program
8000 N Ocean Drive, Dania Beach, FL 33004

This report should be cited as:
Voss et al. 2026. Advancing coral reef research and resilience in southeast Florida: Phase 5. Florida DEP Coral Protection and Restoration Program. Miami, FL. Pp. 1-46.

This report was prepared for the Florida Department of Environmental Protection, Coral Protection and Restoration Program by Florida Atlantic University. Funding was provided by the Florida Department of Environmental Protection Award No.C3D275. The views, statements, findings, conclusions, and recommendations expressed herein are those of the authors and do not necessarily reflect the views of the State of Florida or any of its sub-agencies.

HARBOR BRANCH
FLORIDA ATLANTIC UNIVERSITY
Ocean Science for a Better World®

Manager Summary

This project applied multiple approaches to help understand, reduce, and mitigate coral reef declines in Florida. Continued monitoring of coral condition in the northern portion of Kristin Jacobs Coral Aquatic Preserve (KJCAP) was coupled with genetics to inform coral restoration, coral salinity and thermal stress experiments, and experimental restoration efforts.

Corals in the northern KJCAP areas displayed very little bleaching or signs of disease in 2025-2026.

We've discovered several cryptic lineages across multiple species. Genetic diversity was higher in Florida as compared to Flower Garden Banks , highlighting the importance of species- and region-specific assessments of population connectivity for management and restoration planning.

Acute hyposalinity <20 Practical Salinity Units (PSU) resulted in coral mortality in KJCAP corals, and intermediate salinity stress (~25 PSU) significantly reduced corals' recovery. Survival and recovery of corals can be improved by reducing freshwater discharges, and coral restoration outplanting should be avoided whenever salinity is <25 PSU.

Expanded coral restoration at St. Lucie Reef with transplants from Osborne tire reef maintained >80% survival after two years. For *S. intersepta* and *Siderastrea siderea*, larger transplant colonies had significantly greater survival probability. However, fragment size had no impact on the highly successful *M. cavernosa* transplants.

Resampling Restoration Team Trials corals after ~ 2 years and following the 2023 bleaching event revealed higher than expected survivorship, particularly in KJCAP, and strong evidence of adaptive bleaching in Biscayne and FKNMS.

Acute thermal bleaching among *M. cavernosa* in KJCAP occurs near 4 Degree Heating Weeks (DHW), with marginally increased resilience under chronic thermal stress. These data allow better bleaching predictions in KJCAP based on thermal stress and accumulated DHW.

Through DEP support, we have produced 25 peer-reviewed publications with 5 more in review. DEP support has contributed to 14 graduate degrees, several of whom now serve in state and federal agencies.

Acknowledgements

We appreciate the collaboration with Florida Department of Environmental Protection's Coral Protection and Restoration Program (DEP CPR) who supported this research. We thank the DEP CPR staff, particularly Kathleen Czaia and Maurizio Martinelli for coordinating this award and providing critical suggestions to improve the quality and impact of the project. Jimmy Nelson, Matt Roy, and David Heuberger at FAU Harbor Branch provided marina and logistic support. Stephanie Schopmeyer, Lisa Gregg, and Taylor Davis at FWC, as well as Chris Camargo and Salena Alberti with St. Lucie Inlet Preserve State Park, helped to coordinate permitting for this study.

This project leveraged support from NOAA award NA14OAR4320260 to JDV through the Cooperative Institute for Ocean Exploration, Research, and Technology, a Vero Beach Sunrise Rotary Club Dritenbas Memorial Fellowship to Haley Davis, an Indian River Lagoon Graduate Research Fellowship to Gabrielle Pantoni, and an FAU Dean's Fellowship to Olivia Faris.

Samples within St. Lucie Inlet Preserve State Park were collected under permits 10092545, 01221915, 012102115, 0602215, and 08222325 to Joshua Voss. Coral samples collected outside of the park in the Kristin Jacobs Coral Aquatic Preserve were collected under Special Activity License SAL-23-1702-SRP, SAL-24-1702-SRP, SAL-25-1702-SRP.

Contents

1. Background 6
2. Project Description 6
3. Methodology 7
   3.1. Coral Monitoring Surveys 9
   3.2. Coral Population Genetics to Inform Restoration Activities and Management . 9
   3.3. Coral Salinity Threshold Experiments 12
   3.4. Coral Restoration Efforts at St. Lucie Reef 14
   3.5. Restoration Team Trials Algal Symbiont Analyses 15
   3.6. Thermal Stress and Disease 17
   3.7. QA/QC 23
4. Results 23
   4.1. Coral Monitoring Surveys 23
   4.2. Coral Population Genetics to Inform Restoration Activities and Management 24
   4.3. Coral Salinity Threshold Experiments 30
   4.4. Expanding Coral Restoration Efforts on St. Lucie Reef 33
   4.5. Restoration Team Trials Algal Symbiont Analyses 36
   4.6. Thermal Stress and Disease 41
5. Preliminary Conclusions 42
6. Recommendations 44
7. Literature Cited 46

1. BACKGROUND

Florida's coral reefs recently experienced both a multi-year outbreak of a coral disease described as stony coral tissue loss disease (SCTLD), and significant thermal stress leading to widespread coral bleaching in some southern areas. While coral disease outbreaks and bleaching are not unprecedented, these events are unique due to 1) the presence of multiple symptoms and etiologies that have affected at least 21 species of coral across Florida's Coral Reef (FCR), 2) the persistence of the disease over multiple years, 3) the high levels of mortality associated with infections, and 4) the breadth and prevalence of bleaching in the Florida Keys. SCTLD is highly prevalent and is estimated to have resulted in the mortality of millions of corals across southeast Florida, Biscayne National Park, and the Florida Keys National Marine Sanctuary (FKNMS). Compounding SCTLD and thermal stress effects, freshwater discharge impacts have been particularly acute on coral reefs in Martin County. The work herein focuses on southeast Florida (SE FL) within the Kristin Jacobs Coral Aquatic Preserve (KJCAP) and is part of a larger effort to understand the impacts of disease on coral health in this region and to determine optimized mitigation efforts that may better protect and restore our coral reef resources.

2. PROJECT DESCRIPTION

This project includes multiple complementary approaches to understand, reduce, and mitigate coral reef ecosystem declines in SE Florida. Our major effort was to extend ongoing monitoring of coral reef health and status in the northern section of Florida's Coral Reef. In addition, this project was designed to improve understanding of the current spatial extent of the disease outbreak, prevalence, and species affected. Our objectives included:

- Quarterly monitoring in Martin and Palm Beach counties.
- Building critical data on population genetics and connectivity in Palm Beach, Martin, and northern Broward counties to support restoration planning for coral and sponge species.
- Assessment of coral salinity thresholds to inform freshwater management in Florida, including impacts of hyposalinity stress on coral tissue growth.
- Coral restoration efforts in St. Lucie Inlet Preserve State Park including monitoring transplanted corals from Broward County tire reefs.
- Continue algal symbiont investigation for Restoration Team Trial corals including analyses and comparisons of sequence data.
- Evaluating the cumulative and potentially synergistic effects of thermal stress and disease among corals in SE Florida.

The outcomes of this project contribute to ongoing and future coral management and restoration approaches. Furthermore, this project provides key information for coral species stock enhancement efforts to ensure that restoration efforts maintain community and population-level biodiversity in South Florida.

3. METHODOLOGY

Tables 1-3 below summarize the operational activities at each of our project sites in this period of performance. Project sites, as shown in Figure 1, were chosen in concert with DEP management input from long-term monitoring sites in our lab with over 10 years of survey data at St. Lucie Reef. SEFL sites in Palm Beach County with the highest stony coral cover were selected from a larger number of Hurricane Irma impact survey sites used in 2017 to allow for a continuous monitoring time series in these locations. Broward County sites were chosen due to their relatively high stony coral and SCTLD abundance and to complement annual Southeast Florida Coral Reef Evaluation and Monitoring Program surveys.

Table 1. FAU Harbor Branch Project Quarterly Monitoring Sites. Pompano sites were previously monitored by FAU HBOI since 2017, but in this project year, DEP took on quarterly monitoring efforts.

Location	Site Name	Lat	Long	County
St. Lucie Reef	SLR Central	27.13166667	-80.1340333	Martin
St. Lucie Reef	SLR Ledge	27.12143333	-80.1275	Martin
St. Lucie Reef	SLR South	27.11186667	-80.12551667	Martin
Jupiter	SEFL-4	26.94370833	-80.02197167	Palm Beach
Jupiter	SEFL-5	26.927445	-80.0301	Palm beach
Jupiter	SEFL-6	26.897735	-80.01638333	Palm Beach
Breakers/WPB	SEFL-8	26.71043333	-80.01581667	Palm Beach
Breakers/WPB	SEFL-11	26.6785	-80.01825	Palm Beach
Breakers/WPB	SEFL-12	26.65238667	-80.02068167	Palm Beach
Pompano*	T328	26.17611	-80.09388	Broward
Pompano*	BC1	26.14758	-80.0961	Broward
Pompano*	FTL4	26.13661	-80.09738	Broward

Table 2. FAU Harbor Branch Restoration Sites

Restoration Team Trials with FWC et al.

Location	RTT Site Name	Established	Lat	Long	County
St. Lucie Reef	1-1 Array	4/26/21	27.13121	-80.13388	Martin
St. Lucie Reef	1-1 Control	5/7/21	27.13167	-80.13403	Martin
St. Lucie Reef	1-2 Array	4/21/21	27.1116	-80.12532	Martin
St. Lucie Reef	1-2 Control	5/7/21	27.111867	-80.125517	Martin
Breakers/WPB	1-3 Array	4/16/21	26.71082	-80.01603	Palm Beach
Breakers/WPB	1-3 Control	5/12/21	26.71043	-80.015817	Palm Beach
Breakers/WPB	1-4 Array	4/16/21	26.67856	-80.01797	Palm Beach
Breakers/WPB	1-4 Control	4/16/21	26.67881	-80.01807	Palm Beach

SLR Tire Coral Transplant Site

Location	Site Name	Lat	Long	County
St. Lucie Reef	SLR Central	27.13074	-80.13347	Martin

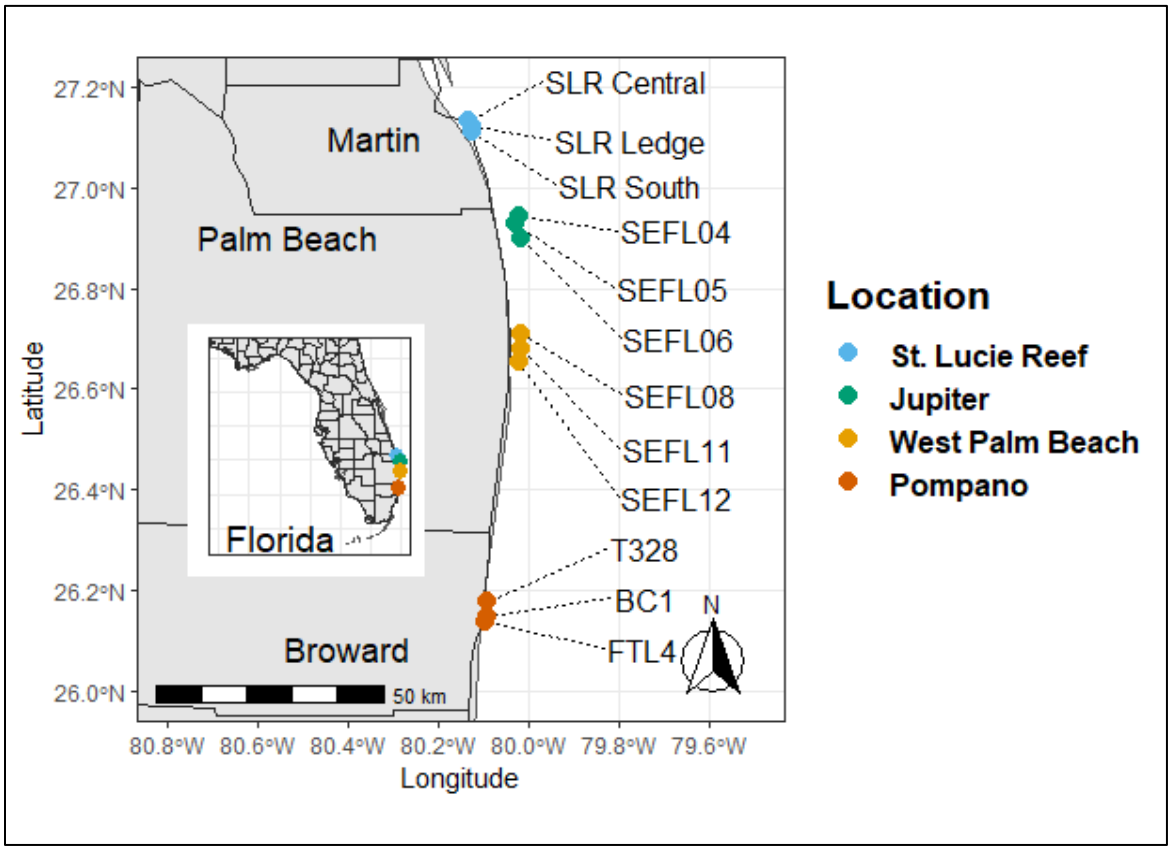

Figure 1. Map of study locations throughout Florida's Northern Coral Reef.

3.1. Coral Monitoring Surveys

Quarterly roving diver disease surveys (see Table 2) similar to Disease Response Monitoring (DRM) surveys were conducted to assess the greatest reef area possible, quantifying disease prevalence over an estimated range of 1000–2000 m^2 per survey based on conditions, principally underwater visibility. Scientific divers swam for 20 min and recorded the coral species and disease status of every living coral colony ≥10 cm in diameter. From the data, SCTLD incidence and prevalence, species diversity, and species richness were calculated. To assess multivariate variation in disease prevalence among sites and survey times, a permutational analysis of variance was conducted in the R package *vegan*. Sites include those continuously surveyed by the Voss lab since 2017.

Table 3. Operational Activities by Site

	Date	Central	Ledge	South
St. Lucie Reef	8/14/25	RD Survey & Transplant Monitoring	RD Survey	RD Survey
St. Lucie Reef	11/18/25	RD Survey & Transplant Monitoring	RD Survey	RD Survey
St. Lucie Reef	2/13/2026	RD Survey & Transplant Monitoring	RD Survey	RD Survey
St. Lucie Reef	5/8/2026	RD Survey & Transplant Monitoring	RD Survey	RD Survey
	Date	SEFL-04	SEFL-05	SEFL-06
Jupiter	8/27/2025	RD Survey	RD Survey	RD Survey
Jupiter	11/14/2025	RD Survey	RD Survey	RD Survey
Jupiter	2/12/2026	RD Survey	RD Survey	RD Survey
Jupiter	6/9/2026 (pending)	RD Survey	RD Survey	RD Survey
	Date	SEFL-08	SEFL-11	SEFL-12
Palm Beach	8/28/2025	RD Survey	RD Survey	RD Survey
Palm Beach	11/17/2025	RD Survey	RD Survey	RD Survey
Palm Beach	2/20/2026	RD Survey	RD Survey	RD Survey
Palm Beach	5/7/2026	RD Survey	RD Survey	RD Survey
	Date	FTL4	BC1	T328
Lauderdale	10/20/2025	RD Survey	RD Survey	RD Survey
Lauderdale	12/1/2025	RD Survey	RD Survey	RD Survey
Lauderdale	3/11/2026	RD Survey	RD Survey	RD Survey
Lauderdale	5/6/2026	RD Survey	RD Survey	RD Survey

3.2. Coral Population Genetics to Inform Restoration Activities and Management

During this period of performance, we focused on analyses of *Stephanocoenia intersepta* and *Xestospongia muta* across the entire Florida Coral Reef and in comparison to sites in across the Gulf of Mexico. For all the *S. intersepta* and *X. muta* samples, ~2-5 cm^2 tissue biopsies were collected and preserved in either Trizol or Zymo DNA/RNA Shield. The samples were extracted using a modified dispersion buffer/phenol–chloroform-isoamyl alcohol extraction and cleaned using the Zymo DNA Clean and Concentrator Kit. DNA

extracts were digested with BcgI enzyme and 2bRAD libraries were prepared following Wang et al. (2012) including some modifications to optimize the libraries. Notably, 12 uniquely indexed 3' adaptors were incorporated, allowing 12 sample ligations to be pooled prior to amplification. Fully degenerate 5' adapters were also included, allowing PCR duplicate removal from downstream analyses. Additionally, triplicate libraries were prepared for three samples and used as a sequencing quality check and to identify natural clones. Sequencing was conducted on an Illumina NovaSeqS1 flow cell at the University of Texas at Austin's Genome Sequencing and Analysis Facility.

Returned sequencing reads were demultiplexed, deduplicated, filtered and trimmed with custom perl scripts and CUTADAPT v3.4. Sample reads were aligned to the *X. muta* reference genome with BOWTIE2 v1.2.2. As there was no *S. intersepta* genome available we employed a de novo reference analysis pipeline. Reads from each sample were first aligned to a concatenated Symbiodiniaceae reference consisting of representative genomes for four genera (*Symbiodinium, Breviolum, Cladocopium, and Durusdinium*) using BOWTIE2 v1.2.2. After excluding the Symbiodiniaceae aligned reads, resulting high-quality reads were used to create a de novo RAD tag reference assembly for *S. intersepta* consisting of clustered (91% similarity) unique sequences found in at least 10% of all samples using custom perl scripts and CD-HIT v4.8.1 (Fu et al., 2012). Potential contamination sequences were removed from the clustered sequences with KRAKEN2 (standard KRAKEN database with added Symbiodiniaceae genomes) and remaining RAD tags were concatenated into a de novo reference and formatted as 30 equally-sized pseudo-chromosomes to be used for mapping. Sample reads were aligned to the de novo reference with BOWTIE2 v1.2.2. The program ANGSD v0.933 was used to determine SNP loci from sequencing reads, generate genotype likelihoods, and create an identity-by-state (IBS) matrix. SNP loci underwent stringent filtering, requiring a minimum mapping quality of 20, minimum base quality score of 30, minimum allele frequency of 0.05, minimum p-value of 10-5 for deviation from Hardy-Weinberg equilibrium, minimum p-value of 10-5 for strand bias, p-value of 10-5 for heterozygosity bias, remove triallelic SNPs, p-value that a locus is variable of 10-6, and had to be present in ≥ 75% of samples. No clonal multi-locus genotypes were identified through hierarchical clustering using an IBS threshold determined by the technical triplicate samples. Two of each of the three technical replicates were removed and ANGSD was run on the clone-free sample set with the previously described filters.

Principal component analysis based on IBS distances was conducted using pcangsd. Then ngsadmix was used to calculate population structure models for cluster values from K = 1–11. In addition to calculating clusters with pcangsd, the most likely value of K was evaluated using the Evanno method through Clumpak.

Genetic connectivity between sampled sites was measured through recent migration rate estimates (immigrant individuals from the previous 2–3 generations) with the BA3SNP function of the program BAYESASS v3.0.4.2. Ten independent runs were conducted with random start seeds for 30 million Markov-Chain Monte Carlo (MCMC) model simulations with a 10 million burn-in and 1000 run sampling frequency. Mixing parameters were adjusted to allow adequate mixing within model runs (acceptance rates = 0.2–0.6). Trace files from independent runs were visualized with TRACER v1.7 to ensure model convergence and consistency between independent model runs. Bayesian deviance was calculated for each independent run and the run with the lowest deviance was used for further analysis. Migration rate estimates (m) were calculated as the mean of the posterior distribution and their uncertainty as 95% high posterior density (HPD) intervals.

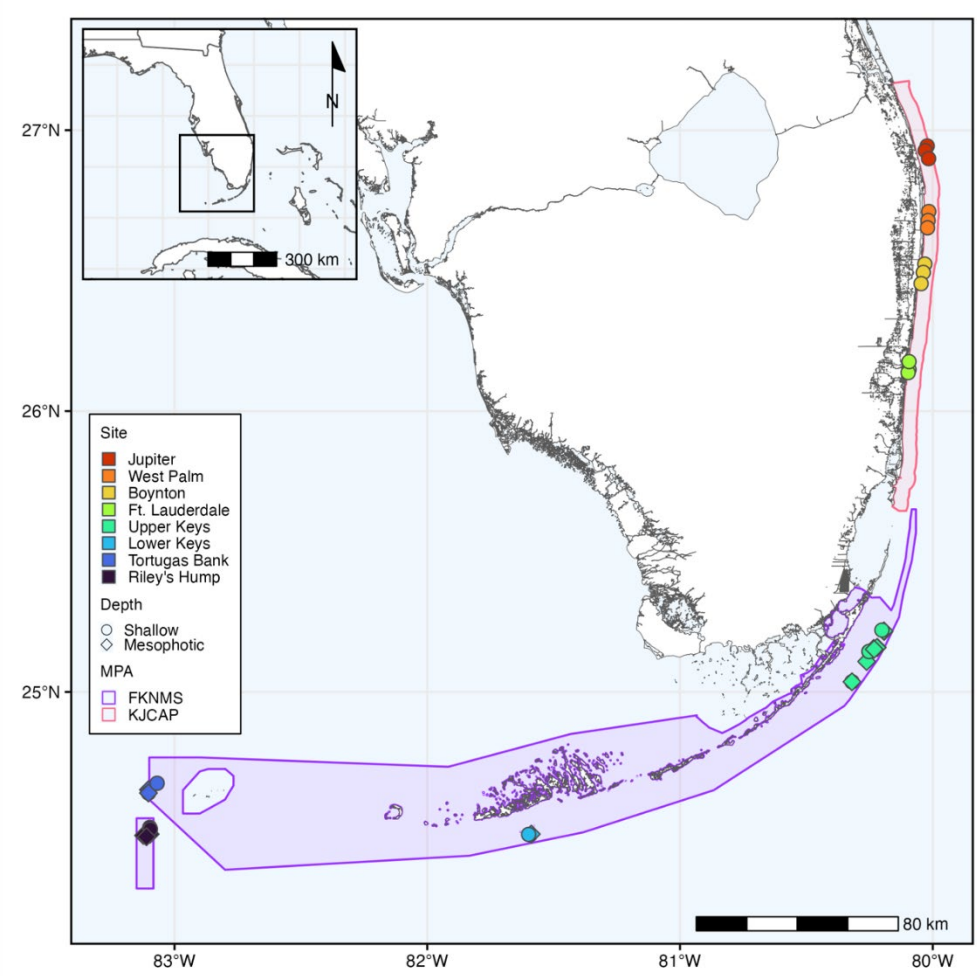

Figure 2. Collection locations for *Stephanocoenia intersepta* and *Xestospongia muta* population genetics and connectivity assessment in the KJCAP and FKNMS.

3.3. Coral Salinity Threshold Experiments

To evaluate the effects of hyposalinity stress on the wound healing responses of *Montastraea cavernosa*, we completed 3 experimental trials: acute hyposalinity stress, chronic hyposalinity stress, and chronic hyposalinity with wounding. A fourth trial, chronic hyposalinity plus SCTLD, was not successful as the donor SCTLD colonies appeared not infectious. This period of performance focused on final data analyses, interpretation, and manuscript preparation.

Coral collections for all experiments took place over a series of three dives in West Palm Beach where 10 colonies of *Montastraea cavernosa* were collected. Sub-samples were collected and preserved in DNA shield and Trizol for potential future molecular analyses. Colonies were transported in coolers to Harbor Branch where they recovered for 48 hours prior to fragmentation. Corals cut into 3x3 cm fragments using a diamond blade tile saw and glued to labeled limestone tiles.

At the initiation of the experiment, 6 fragments from each of the 8 *M. cavernosa* genets were visually ranked by size and haphazardly sorted into one of 6 tanks, with one representative of each genotype in each tank. To prevent confounding variables, the positions of the fragments within the tank were randomized, ensuring that orientation did not introduce any bias.

Experiment 1: Acute Hyposalinity Tolerance Threshold

Each experiment was initiated with an acclimation period in which all six aquaria were held at a control salinity of 35 PSU for five days (day -5 to -1, Figure 3). The salinity in experimental aquaria was then reduced by 2 PSU/day continuously. Each day, 20% water changes took place in each tank, maintaining 35 PSU in control tanks and reducing the salinity of experimental tanks daily until the termination of the experiment (Figure 2).

Experiment 2: Intermediate-Hyposalinity Tolerance Duration (Chronic Exposure)

Based on mortality and health scores in the acute hyposalinity experiment, 25 PSU was selected as the intermediately stressful salinity for the following experiments. After the same acclimation phase, the salinity in three experimental tanks was reduced to and maintained at an intermediately stressful salinity of 25 PSU utilizing 20% water changes. During the “drop” phase, the treatment tanks underwent a continuous drop in salinity by 2 PSU (days 1–5), until reaching and being maintained at 25 PSU (days 6–26).

Experiment 3: Chronic Hyposalinity + Wound Healing

This study utilized 8 remaining colonies of *M. cavernosa* in an effort to better understand hyposalinity impacts on recovery rates of damaged corals. The same procedures outlined above in Experiment 2 were repeated, with the addition of inflicting artificial tissue wounds on the day that treatment tanks reached 25 PSU. Every fragment in both the control and intermediate hyposalinity treatment received a single wound in the center of the fragment using a ¼" diameter, cylinder end, tungsten carbide burr bit in a drill press set to a ¼" depth stop into the coral tissue.

Each day, images were taken of the fragments, and additional photos were taken directly following manual agitation to cause polyps retraction and create better visibility of the wound. At ten time points (days 1, 5, 10, 15, 20, 25, 30, 35, 40, and 45) retracted-polyp photos were lens-corrected using Photoshop (2022), and then traced in Image J to calculate wound size in cm^2. A small plastic ruler was placed at the bottom of the tank to scale each image. This experiment ended after 45 days, allowing for several control fragments to reach 100% healed. Fragments were given a qualitative health assessment each day by adopting a physical scoring system from Woodley and Downs (2014). These "physio-scores" were compiled by examining the following attributes: coloration, tissue integrity, and polyp activity. Each frag received three scores, one for each category; scores ranged from 5 (best possible score) to 1 (worst possible score). Coloration ranking was based on tissue bleaching, where normal color received a 5 and completely bleached tissue received a 1. The scoring system for tissue integrity was adapted slightly to fit the parameters of this study; a fully healed fragment received a 5 and all wounded fragments received a 4. Additionally, any tissue loss observed after drilling was scored accordingly. A perfect activity score of 5 was given to polyps that were fully extended, while the lowest score of 1 was given to fragments with sunken and retracted polyp bodies.

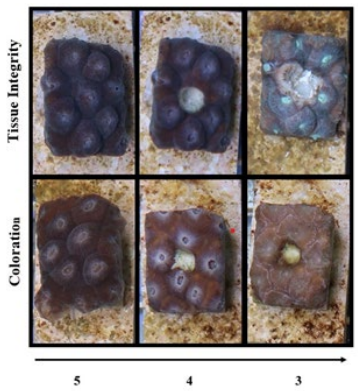

Figure 3. Coloration and tissue integrity ranges observed throughout the experiment are represented above.

Scaled images were taken daily and all photos taken were lens-corrected to eliminate underwater distortion caused by optical refraction. New tissue growth (cm^2) following artificial wounds was calculated using ImageJ based on the protocol developed by the Restoration Team Trials project (Pantoni 2023). Each fragment was traced at 10 different time points, beginning at injury infliction (day 1) and concluding on day 45 after 41.6% of fragments from control tanks were healed.

Each day after health scoring and images were taken, all aquarium temperatures and salinities were recorded to ensure stable parameters were maintained. After data collection had concluded, every tank received a 20% water change (18 L) daily maintaining either 25 PSU for the treatment tanks or 35 PSU for the control tanks. Transparent lids covered each tank to reduce evaporation and maintain temperature.

All statistical analysis was completed in RStudio using the package ggplot2 for data visualization (v3.3.3; Wickham, 2016). Area values of coral wounds obtained from Image J tracing represented the raw surface area of the lesion, with 0 cm^2 given to fragments that had completely healed. A repeated measures analysis of variance (RM ANOVA) was run on area tissue growth comparing tank and treatment over ten time points at 5-day intervals (days 1-45). RM ANOVAs were used to analyze health score data individually with each parameter (color, tissue integrity, and polyp activity) over time. In order to determine which group means showed significance, post-hoc pairwise comparisons were performed using the Bonferroni correction method.

3.4. Coral Restoration Efforts at St. Lucie Reef

St. Lucie Reef was identified as a target for additional coral restoration based on the success of previous outplants in the Restoration Team Trials (RTT) study. We identified a site for this transplantation study that is in close proximity to the RTT outplant site at SLR Central, which had strong outplant survival and growth. The depth at this site is about 3.5m and the bottom composition is mainly worm rock. Corals of three target species, *Montastraea cavernosa*, *Siderastrea siderea*, and *Stephanocoenia intersepta* were collected from the relic tire artificial reef off the coast of Ft. Lauderdale, FL by David Gilliam and his lab at NSU. They held the corals in their *in situ* nursery until we retrieved all 64 colonies and transplanted approximately 10 small (4-7 cm diameter) and 10 large (>10 cm diameter) individuals of each species. The corals were transplanted onto St. Lucie Reef on 26 February 2024. We used coral anchor cement in piping bags to attach each colony to the reef and assigned a numbered (701-764) cattle tag nailed into the reef. After transplanting, each colony was photographed using a Olympus TG-6 camera mounted on a fixed and scaled PVC stand so that each photo is the same distance above each colony (Figure 4).

During each monitoring interval, we continued to photograph and take notes on the status of each colony. The notes include any signs of disease, bleaching, predation, algal overgrowth, and sediment smothering on the transplants. The percent of surviving colonies of each species within each size class was calculated for each monitoring interval (initial outplanting to 27-months). To compare probability of survival between size classes for each species, we created Kaplan-Meier survival curves and then used log-rank tests to identify any significant differences between the curves.

Using the photos taken at each monitoring interval, we monitored growth of the transplants by calculating changes in live tissue surface area over time. Images were uploaded to ImageJ, scaled, and two-dimensional surface area was traced using a Wacom CTL472K1A One tablet with stylus. Percent change in surface area was calculated from starting colony size to the size at each traced monitoring interval. A mixed analysis of variance (ANOVA) was used to identify significant differences in percent change in surface area between species, size classes, and across time.

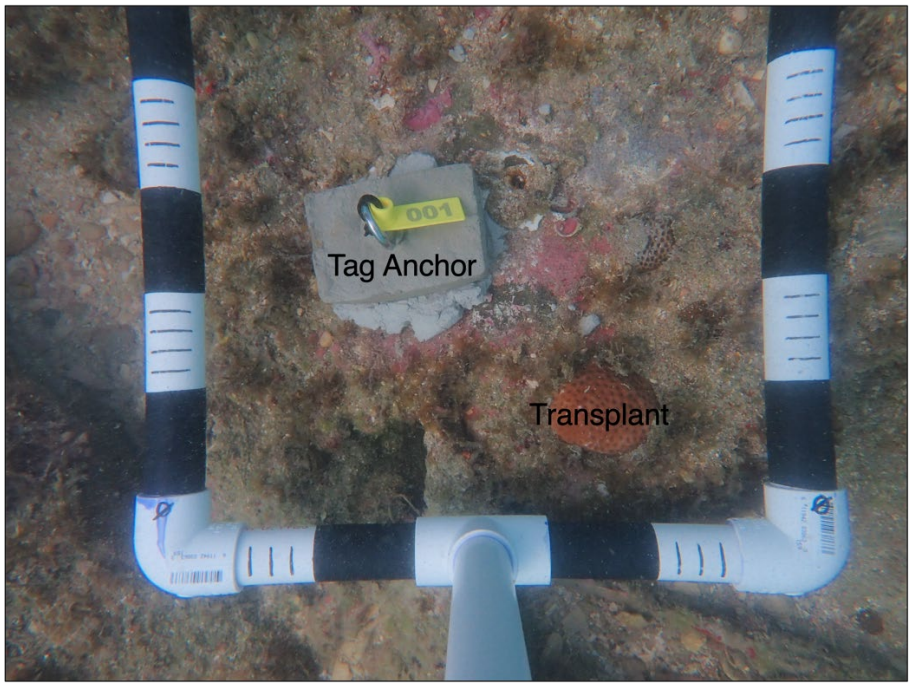

Figure 4. Image of *Siderastrea siderea* transplant colony #001 (previously #701) with new tag anchor and tag number.

3.5. Restoration Team Trials Algal Symbiont Analyses

A sampling protocol for evaluating algal symbiont structure within the RTT outplants was created by HBOI and shared with all partners to ensure sampling was conducted consistently across the 6 regions. Biopsies were taken using a hammer and 3/8" diameter round leather punch from the center of the colony or the center of the largest fragments if not all fragments were fused (Figure 6). Each biopsy was transferred into a labeled plastic

bag underwater and leather punches were cleaned with a wire brush between colonies. The colony number and corresponding sample bag number were recorded on a datasheet. Once a leather punch became chipped after several uses, a new punch was used. After each dive, samples were transferred from the labeled plastic bags into labeled 15 mL falcon tubes filled with Zymo DNA/RNAshield. The sample tube number and corresponding colony number were also recorded onto the datasheet used during underwater sampling.

Tissue biopsy samples were collected from all living coral outplants by RTT partners in their respective regions for Timepoint 2 between 15 May 2023 and 14 June 2023 at the end of the project's 2-year monitoring period, and then for Timepoint 3 between 11 Jan 2024 and 27 Feb 2024, following the 2023 bleaching event that impacted areas in Florida from Miami south. Once the samples were collected, they were delivered to HBOI, categorized by region, and put into the –80° C freezer for storage until extraction.

DNA was extracted from preserved tissue samples with a modified dispersion buffer/phenol-chloroform-isoamyl alcohol extraction (Sturm, 2020). Extracted DNA was cleaned with a Zymo DNA Clean and Concentrator Kit following the manufacturer's instructions. DNA quality was determined with a NanoDrop 2000 (Thermo Fisher) and dsDNA quantity was measured with a broad-range assay kit on a Qubit 4.0 fluorometer (Thermo Fisher). Extracted DNA was used for symbiont community typing through high-throughput sequencing of the internal transcribed sp*acer* 2 (ITS2) region of ribosomal DNA operon. The Symbiodiniaceae specific primer pair, SYM_VAR_5.8S2/SYM_VAR_REV, was used to target the ITS2 region of Symbiodiniaceae ribosomal DNA operon for sequencing (Hume et al., 2018). Each sample was run in an initial 30 µL PCR containing 20 ng of the template genomic holobiont DNA (Eckert et al., 2020; Klepac et al., 2015). Products from the first PCR were cleaned using a Zymo DNA Clean and Concentrator kit following the manufacturer's instructions. Initial PCR products were quantified with Qubit (Invitrogen) and diluted for a second PCR which incorporated a unique combination of indexed forward and reverse Illumina adapter primers producing a unique dual index or barcode for each sample (Klepac et al., 2015). Each sample was then visualized on a gel to ensure quality before sending out to the sequencing facility. The samples are then pulled and sent for sequencing at The Herbert Wertheim UF Scripps Institute for Biomedical Innovation and Technology. The pulled libraries will be sequenced across three runs on the Illumina MiSeq platform (v3 chemistry) with paired-end 250 bp reads.

Sequencing of algal symbiont DNA from 1,462 coral tissue samples returned an average of 43,800 reads per sample. Raw sequences were submitted to SymPortal for initial filtering and alignment using standard sequence quality control protocols implemented with MOTHUR 1.39.5, the BLAST+ suite of executables, and minimum entropy

decomposition (Hume et al. 2018). Within R Studio, ITS2 type profiles generated by SymPortal were further subsetted by respective coral species and low-abundance ITS2 types were subsequently purged from the dataset. ITS2 types were normalized and sorted based on relative abundances to generate stacked bar plots illustrating Symbiodiniaceae community compositions in each outplanted coral species across restoration region and time point. Symbiodiniaceae genera were further color coded based on within-genus descending abundance (*Symbiodinium* = purple; *Breviolum* = blue; *Cladocopium* = green; *Durusdinium* = red).

The full Symbiodiniaceae *ITS2* sequencing library preparation can be found here: https://ryaneckert.github.io/website/ITS2_protocol/

In this period of performance we focused on SymPortal analyses to quantify changes over regions, species, and time to determine the potential impacts of outplanting and thermal stress on algal symbiont communities within these corals.

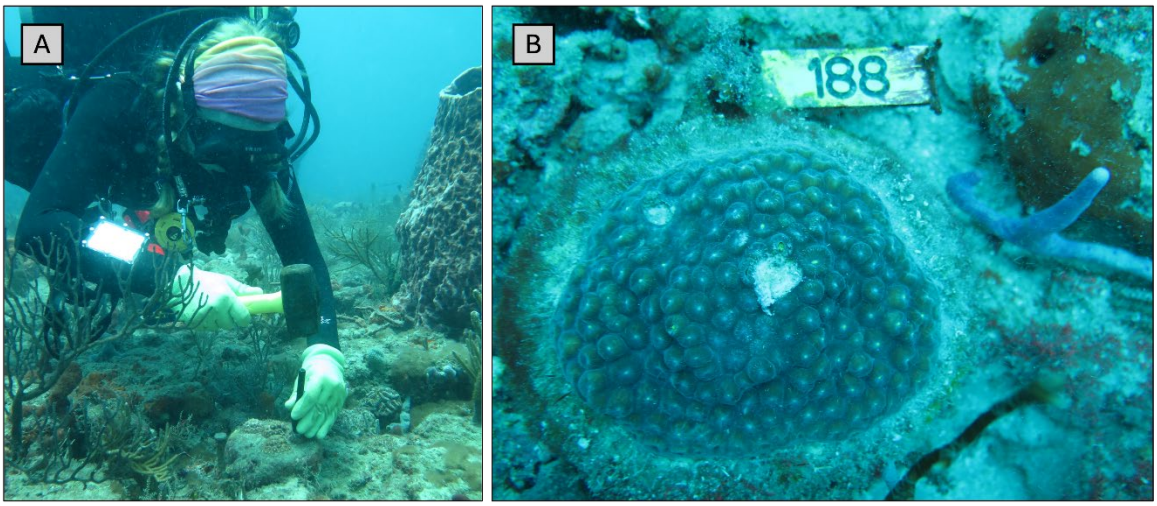

Figure 5. A diver using a 3/8" diameter round leather punch and hammer to collect a tissue biopsy (A), and a colony post-sampling with the tissue biopsy removed (B).

3.6. Thermal Stress and Disease

In June 2025, we collected 12 colonies (30–38cm diameter) of *M. cavernosa* using a from Breakers Reef at 15-17m depth. Sampled colonies were at least 10m apart to minimize potentially sampling clones, visually healthy with normal coloration (no bleaching or paling), no algal growth, no sedimentation, and no observable tissue degradation. After collection, colonies were surfaced and placed in coolers with ambient seawater changes every 10 minutes while being transported to FAU Harbor Branch. Upon arrival, colonies were placed in 3 common holding tanks under ambient conditions (24–26ºC and 34–37ppt) for 2–5 days until fragmentation. Each colony was fragmented into 18 roughly equal pieces

using a diamond blade tile saw and artificial seawater as lubricant. Fragments were an average of 8.24cm^2, ranging from 2.89–14.8cm^2. Individual fragments were glued to 5 x 5 cm natural limestone tiles each with a small colored ceramic tag corresponding to each genotype. The fragments recovered in 6 common holding tanks under ambient conditions (24–26ºC and 34–37ppt) for 1 month, allowing the lesions from fragmentation to heal fully prior to the thermal stress experiments.

Each 76-liter experimental tank contained an electric heater with thermostat (Visitherm model ML90641), one powerhead with filtration attachment (Aquaclear powerhead model A586, Aquaclear filter attachment model A575), one powerhead (Marineland model ML90509), and an LED multispectrum aquarium light (Nicrew model N14584; Figure 6). Temperature and salinity were continuously monitored using Neptune APEX A3 systems and checked daily using a Xylem YSI ProSolo digital water quality meter and refractometer. No significant differences in daily average temperatures were detected between APEX and YSI measurements, therefore continuous APEX measurements were used for data analysis in acute thermal stress experiments, while YSI measurements were used as a complementary monitoring tool. Photographs of each tank were taken daily, with a color scale standard and ruler in each image for scale. Corals were exposed to an average of 91µmol/m/s, as a measure of photosynthetically active radiation (PAR). All tanks were exposed to 12-hour light cycles, turning on at 12:30am and turning off at 12:30pm, so that light-sensitive measurements could be taken during working hours. Throughout all trials, salinity was maintained between 34 and 37ppt.

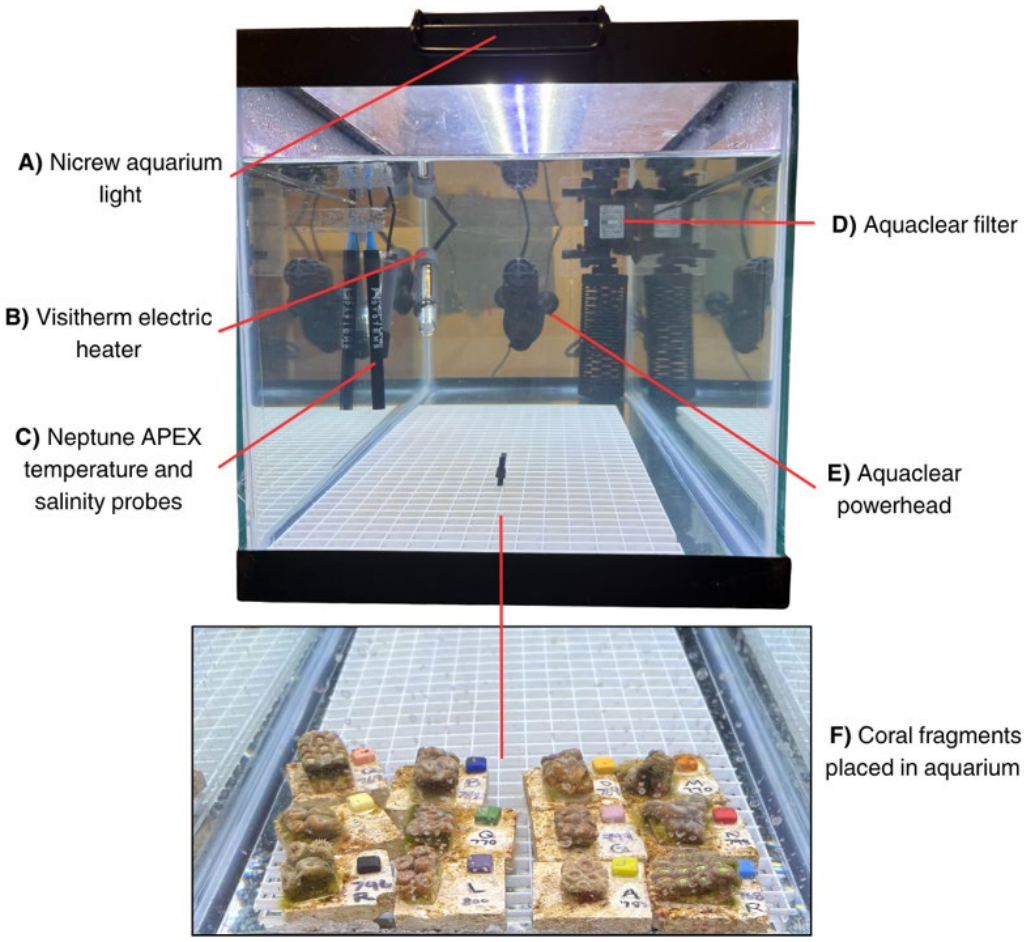

Figure 6: Experimental tank setup. Letters A–E denote equipment in each experimental aquarium. Letter F shows how coral fragments were placed in aquaria. Coral fragments were placed in the front third of each tank to prevent potential damage from powerheads and for ease of daily measurements.

Photosynthetic efficiency was measured through pulse-amplitude modulated fluorometry (PAM) using a Walz Diving PAM Chlorophyll Fluorometer. As corals bleach and expel associated symbionts, the photosynthetic efficiency and the F_v/F_m value will decrease. Bleaching thresholds are commonly quantified using effective dose (ED), defining the percent decline in F_v/F_m. We calculated thermal thresholds of ED30 and ED50. ED50 is widely used across coral studies and represents the upper thermal limit of coral performance (Klepac et al. 2024). This approach quantifies the extent and severity of thermal stress in the coral holobiont's photosystem before a coral is fully bleached and/or dead.

In all thermal stress trials, three control tanks were held under ambient conditions (24–26ºC) for the duration of the experiment (Figure 7). During acute thermal stress trials,

temperatures in three treatment tanks were increased by 1ºC every other day until a temperature of 33.8°C was reached (27 days). Three individual PAM measurements were taken from different locations on each coral fragment, then averaged together for analysis. Three initial measurements were taken 3 days prior to thermal ramp and averaged together as a baseline F_v/F_m value. This baseline F_v/F_m value was set as the maximum photosynthetic efficiency of the coral and standardized to represent 100% photosynthetic efficiency. We conducted PAM measurements every other day throughout the experiment and then every day once measurable thermal stress was induced (when F_v/F_m values began to decline). PAM measurements were collected 1 hour after aquarium lights turned off to allow full relaxation of PSII receptors. All F_v/F_m values for each genotype across experimental tanks were standardized to the baseline F_v/F_m, resulting in percent F_v/F_m declines. In Trial 1, the bleaching threshold was defined as the accumulated experimental degree heating weeks (eDHW) at which the photosynthetic efficiency (F_v/F_m) is reduced by 30%, also known as an effective dose of 30% (ED30). Acute trials were concluded when all coral fragments reached a minimum effective dose of 30 (ED30), when photosynthetic efficiency declined by 30%.

Figure 7: Experimental design for thermal stress experiments. (A) Example photograph of experimental aquarium, including color standard and ruler. Each fragment was superglued to a tile base with a unique colored tile representing each genotype. Fragments received a letter to signify each unique fragment and were randomly arranged in tanks. (B) Experimental design consisted of three tanks in each treatment.

Treatment groups in chronic thermal stress experiments followed acute trials, consisting of three control tanks and three thermal stress tanks. In three chronic thermal stress tanks, temperature was increased by 1°C every other day for 20 days, and held between 29–31°C for 36 days.

The original intent of the chronic thermal stress trials was to elucidate the cumulative impacts of thermal stress and disease. In August 2025, four whole diseased *M. cavernosa* (30–38cm diameter) colonies were identified and collected opportunistically in Jupiter, FL. Collected colonies had active disease lesions consistent with signs of SCTLD. Diseased colonies were transported to HBOI-FAU while being flushed with seawater repeatedly, then placed in separate holding tanks until disease transmission experiments began. Immediately prior to disease being introduced to experimental tanks, diseased colonies were fragmented using a diamond blade tile saw.

The experimental design for the thermal stress and disease trials consisted of twelve tanks; three control, three thermal stress, three disease exposed, and three thermal stress and disease exposed simultaneously. Three control tanks were exposed to ambient temperature and salinity conditions for the duration of the experiment (Figure 8). Three experimental chronic thermal stress tanks were held under conditions mentioned above. The disease exposed group consisted of three tanks held at ambient conditions each with one diseased fragment with an active disease lesion. Finally, the thermal stress and disease group had a temperature increase of 1°C every other day and was held between 29–31°C for the duration of the experiment. In the thermal stress and disease group, once temperatures of 29°C were reached, a diseased fragment was introduced into aquaria (Figure 8). Disease was introduced to aquaria by placing diseased fragments in aquaria near healthy coral fragments, and all diseased fragments were introduced simultaneously. After nine days of disease exposure, a diseased tissue slurry was added to aquaria. Diseased tissue was removed from the coral skeleton using a Water-Pik, then 5mL of tissue slurry was pipetted directly onto each coral fragment. No disease transmission to healthy fragments was observed and after 1 month in aquaria, we elected to conclude the experiment.

Figure 8: Experimental layout for thermal stress and disease experiment. (A) Example photograph of experimental aquarium, including color standard and ruler. Diseased fragment placed behind corals for purposes of photographing all fragments together. After daily photographs were taken, diseased fragment was moved 10 cm upstream of coral fragments. (B) Experimental design consist of three tanks in each treatment, with four treatment groups. (C) Image of coral exposure to disease slurry. Each coral fragment received an equal amount of disease slurry, pipetted directly onto fragment.

3.7. QA/QC

All roving diver and experiment data were entered into Access or Excel where QA/QC and data summaries were performed. Once entered, data were reviewed to ensure consistency with data sheets. During the summary table creation, the data were once again reviewed for consistency between teams especially for coral species and disease identifications. In some cases, site pictures were reviewed to help this QA/QC process. All molecular data were quality checked, filtered, and demultiplexed as described above.

4. RESULTS

4.1. Coral Monitoring Surveys

SCTLD prevalence was very low at all survey regions. There were no observations of SCTLD on St. Lucie reefs and Jupiter reefs. Across all the monitoring regions Ft. Lauderdale reefs continued to have the highest SCTLD prevalence, but still very low, ≤ 1% (Figure 9). From 2017 SCTLD prevalence has significantly decreased between locations and years (PERMANOVA: $P < 0001$). The only species with observed SCTLD at any of our monitoring sites was *Montastraea cavernosa* (Figure 10).

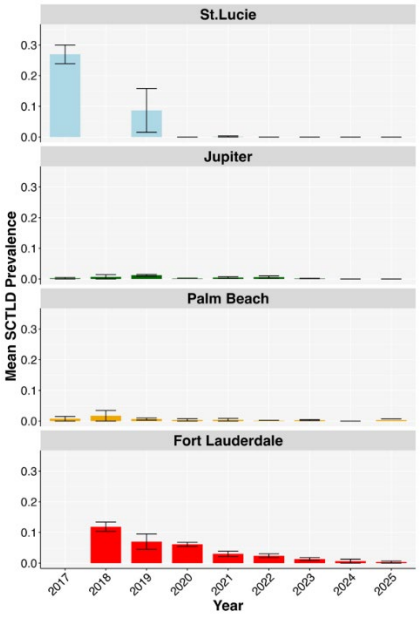

Figure 9. Mean SCTLD prevalence ± SD from roving diver surveys across survey year within each survey region.

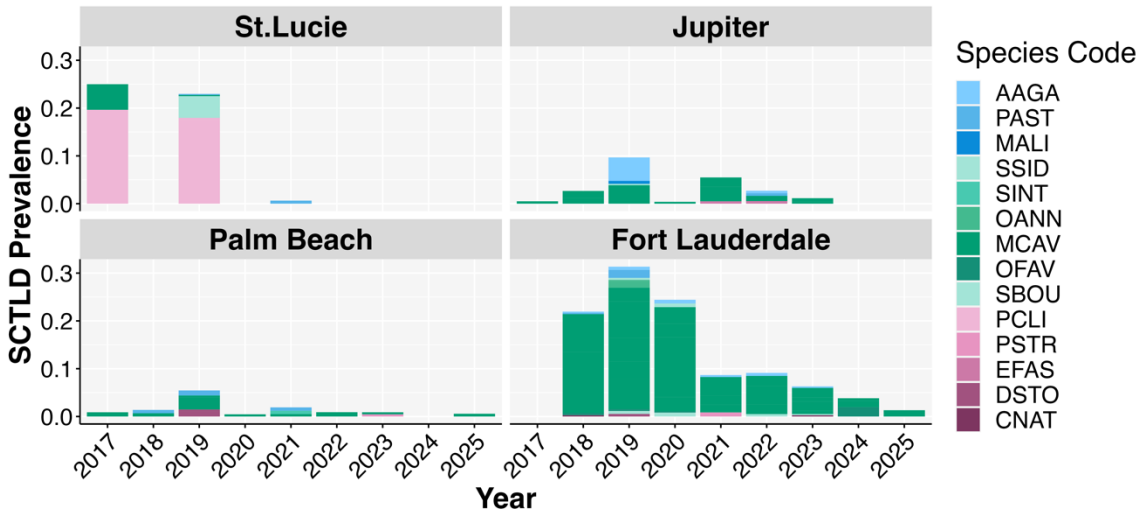

Figure 10. Mean SCTLD prevalence of species affected by SCTLD at each monitoring region across survey years, coral species are color coded by SCTLD susceptibility group. Blue shades represent low susceptible species, green shades represent intermediately susceptible species, and pink shades represent highly susceptible species

4.2. Coral Population Genetics to Inform Restoration Activities and Management

Stephanocoenia intersepta

STRUCTURESELECTOR suggested *K* values of 4 and 5. Based on admixture, dendrogram, and principal components analyses we continued analyzing five cryptic lineages of *S. intersepta* (**Fig. 11**). Very few *S. intersepta* samples were considered admixed for further analyses (3 samples; **Fig. 11D**). Samples from FGBNMS were distinct from most Florida samples (**Fig. 11A, B**). Within Florida, FKNMS and KJCAP samples were fairly distinct from one another, but less so than from FGBNMS samples (**Fig. 11B, C**). Flower Garden Banks samples were exclusively assigned to a single lineage, Si1, while Florida samples were comprised of four cryptic lineages (**Figs. 11A, E, 12D**). Within Florida MPAs, FKNMS sites were dominated by the lineages Si2 and Si4, while the majority of samples from KJCAP belonged to the Si3 and Si5 lineages (**Figs. 11E, 12D**).

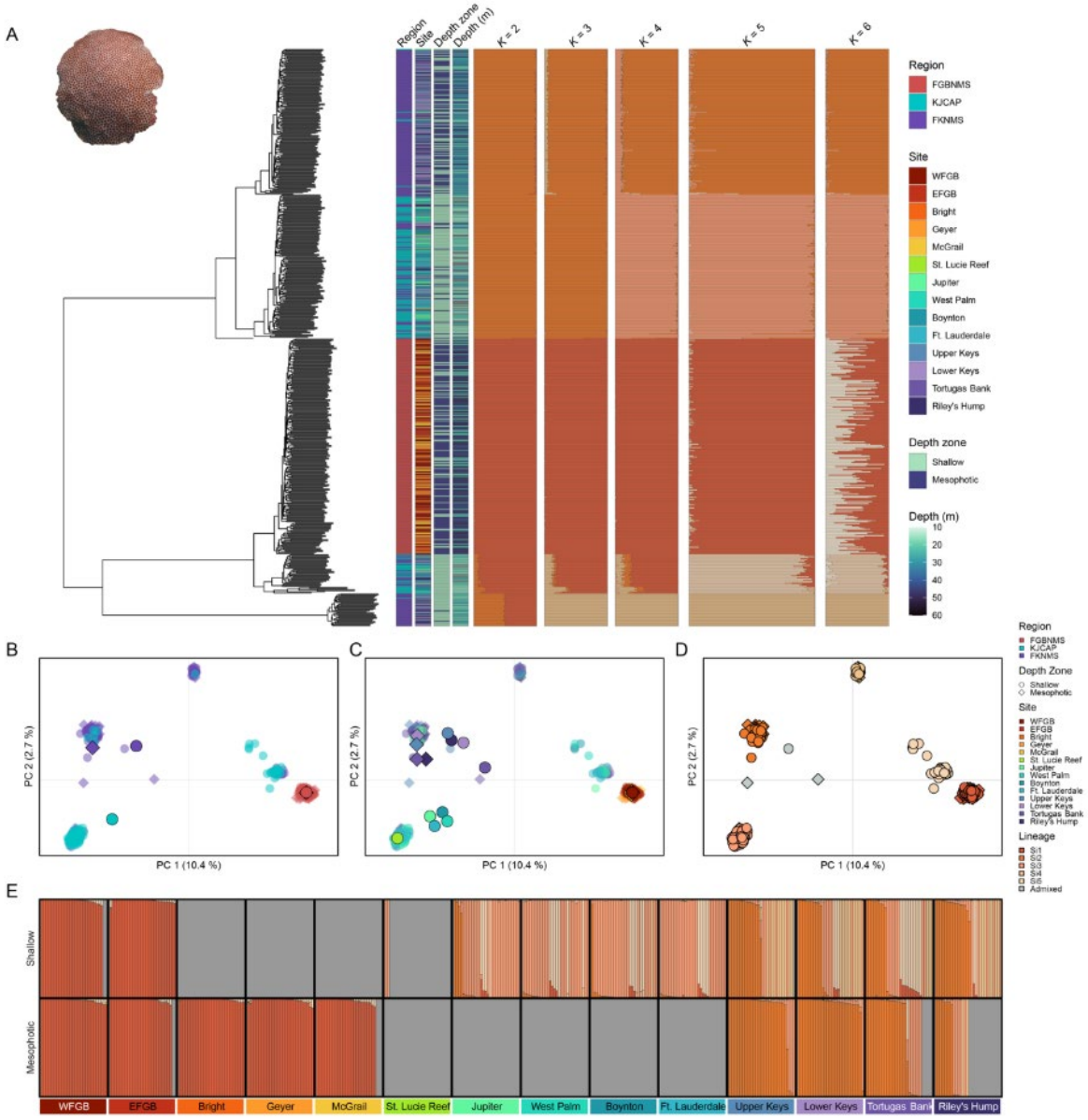

Figure 11. ***Stephanocoenia intersepta*** **population genetic structure. A** Dendrogram of samples based on IBS matrix from ANGSD with matching region, site, depth zone, and depth (m) data and structure plots for K =2–6 for each *S. intersepta* sample. **B** Principal component analysis from PCANGSD, where color represents sampling region and shape represents sampling depth zone. Larger, opaque shapes are sample population centroids and smaller, transparent shapes individual samples. **C** Same plot as **B** and with samples colored by sampling site. **D** Same plot as **B** and **C** with samples colored by lineage assignment from K = 5 data set. **E** Structure plot from NGSADMIX analysis with samples grouped by site and depth zone. Each bar represents an individual sample and the proportion of each color is the probability of membership to that genetic lineage.

There was distinct distribution of lineages across depth (F = 109.41, p < 0.001; **Fig. 12A**) The first three *S. intersepta* lineages (Si1, Si2, and Si3) were found across a broad depth

range, from shallow to mesophotic reefs. The Si4 and Si5 lineages were almost exclusively found in shallow depths (**Fig. 12A**). Genetic differentiation varied widely among lineages (F_{ST} = 0.046–0.23; **Fig. 12F**). The FGBNMS lineage, Si1 was least differentiated from the Si5 lineage (F_{ST} = 0.05). The Si2 and Si3 lineages were also among some of the least differentiated lineages (F_{ST} = 0.046).

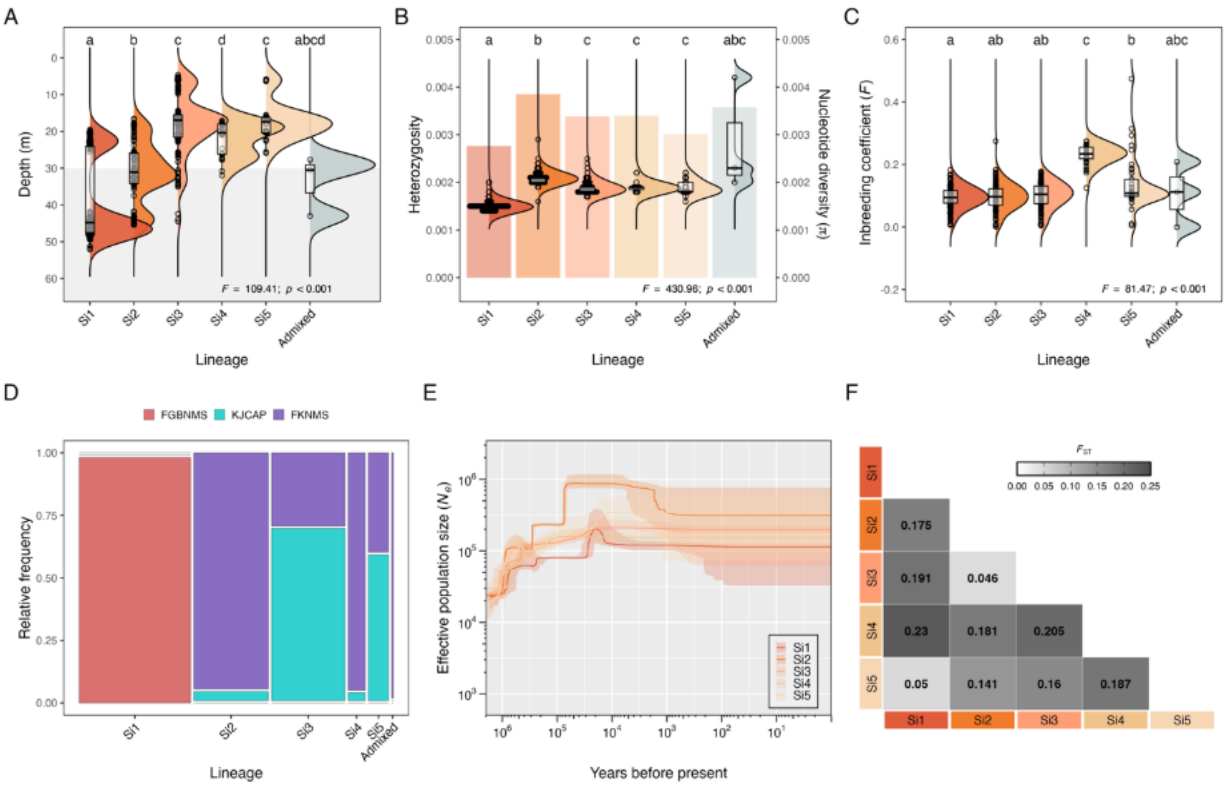

Figure 12. *Stephanocoenia intersepta* lineage diversity and demographics. A *S. intersepta* lineage depth distribution. Shaded portion of graph indicates mesophotic depths. **B** Lineage heterozygosity across variant and invariant loci. Transparent bars behind violins represent nucleotide diversity (π) for each lineage. **C** Mean inbreeding coefficient by lineage. Letters indicate significant differences among lineages and Welch's ANOVA results are listed in **A**, **B**, & **C**. **D** Distribution of lineages across regions. Color of bars corresponds to sampling region. Width of bars is indicative of the relative proportion of samples assigned to that lineage. **E** Lineage effective population size through time. X-axis is thousands of years ago (KYA). Bounding ribbons are 75% confidence intervals. Note log scale for axes. **F** Pairwise fixation index (F_{ST}) heatmap among lineages. Darker coloration indicates higher F_{ST}.

Genetic diversity also varied among *S. intersepta* lineages (**Fig. 12B, C**) Heterozygosity was lower in the FGBNMS Si1 lineage, on average and highest, on average, in Si2, the major depth-generalist lineage in FKNMS (**Fig. 12B**). These same patterns are reflected in the nucleotide diversity (π) of these lineages (**Fig. 12B**). On average, inbreeding was greater in the shallowest Florida lineages (Si4, Si5) with the greatest inbreeding in Si4 (**Fig. 12C**). All other lineages exhibited fairly low inbreeding levels on average (**Fig. 12C**). Effective population size of varied widely among *S. intersepta* lineages and

throughout time (**Fig. 12E**). The FGBNMS lineage (Si1) has historically had one of the lowest effective population sizes, consistent with the constrained genetic diversity estimates we found in FGBNMS. Conversely the predominant, depth-generalist lineage in FKNMS (Si2) has remained one of the largest effective population sizes throughout time (**Fig. 12E**). All lineages experienced large population expansions followed by population contractions, though the scale of this flux was greatest in the FKNMS depth-generalist lineage, Si2 (**Fig. 12E**).

Xestospongia muta

STRUCTURESELECTOR selected *K* values of 7–9, with the majority of selection methods suggesting *K* = 7. Based on STRUCTURESELECTOR results, dendrogram, and admixture analyses we continued to analyze *X. muta* as seven cryptic lineages (**Fig. 13A**). Within FGBNMS and Florida there were multiple cryptic lineages found (**Figs. 13A, B, E**). In FGBNMS samples predominantly assigned to one of three lineages and were distinct from most Florida samples, as evidenced by PCA (**Figs. 13A, B, C, D**). Within Florida, X. muta populations were largely similar across MPAs and sampling sites, with the exception of Ft Lauderdale which hosts a small population of genetically distinct *X. muta* not found in our other sampling sites. Population structure differed more across depth in FGBNMS than in FKNMS (**Figs. 13C, E**).

Xestospongia muta lineages exhibited distinct distribution across depth (**Fig. 14A**). There were several lineages which were predominantly found on either mesophotic or shallow reefs, as well as several depth-generalist lineages. Admixed samples were found with a wide distribution across all depths (**Fig. 13A**). Lineages were also distinctly distributed across regions, with FGBNMS comprised of three lineages (**Fig. 14D**) not found in either FKNMS of KJCAP (**Fig. 14D**). The four lineages found across Florida (**Fig. 14D**) were found across both MPAs and the majority of admixed *X. muta* were found in Florida (**Fig. 14D**). Differentiation among lineages varied (F_{ST} = 0.013–0.186; **Fig. 14F**). The lineage at Ft. Lauderdale (Xm5) was among the most differentiated lineages from all other lineages (F_{ST} = 0.128–0.186; **Fig. 14F**). The leas differentiated lineages were Xm3:Xm7 and Xm1:Xm6 (F_{ST} = 0.013 and 0.028, respectively; **Fig. 14F**), which were both comparisons of lineages found within a region (Florida and FGBNMS, respectively; **Fig. 14D**).

Heterozygosity also varied among lineages, though overall was lower than in *S. intersepta* lineages. The Ft. Lauderdale lineage, Xm5 had significantly higher heterozygosity and nucleotide diversity than any other lineage or admixed samples (**Fig. 14B**). There was a significant difference in inbreeding among lineages, though there were no strong trends between FGBNMS and Florida lineages, with most lineages containing a large distribution of inbreeding (**Fig. 14C**). Throughout history, X. muta lineages have

fluctuated in effective population size (**Fig. 14E**). The FGBNMS lineages (Xm1, Xm4, Xm7) had some of the lowest effective population sizes in the recent past, with only the relatively small Xm5 lineage from Ft. Lauderdale having a smaller effective population size than Xm4 (**Fig. 14E**). While the relative population sizes vary among lineages, most lineages experienced a period of growth and stasis followed by a decline to recent effective population sizes (**Fig. 14E**). However, two lineages in Florida, Xm2 and Xm7 have remained relatively stable following past periods of expansion (**Fig. 14E**).

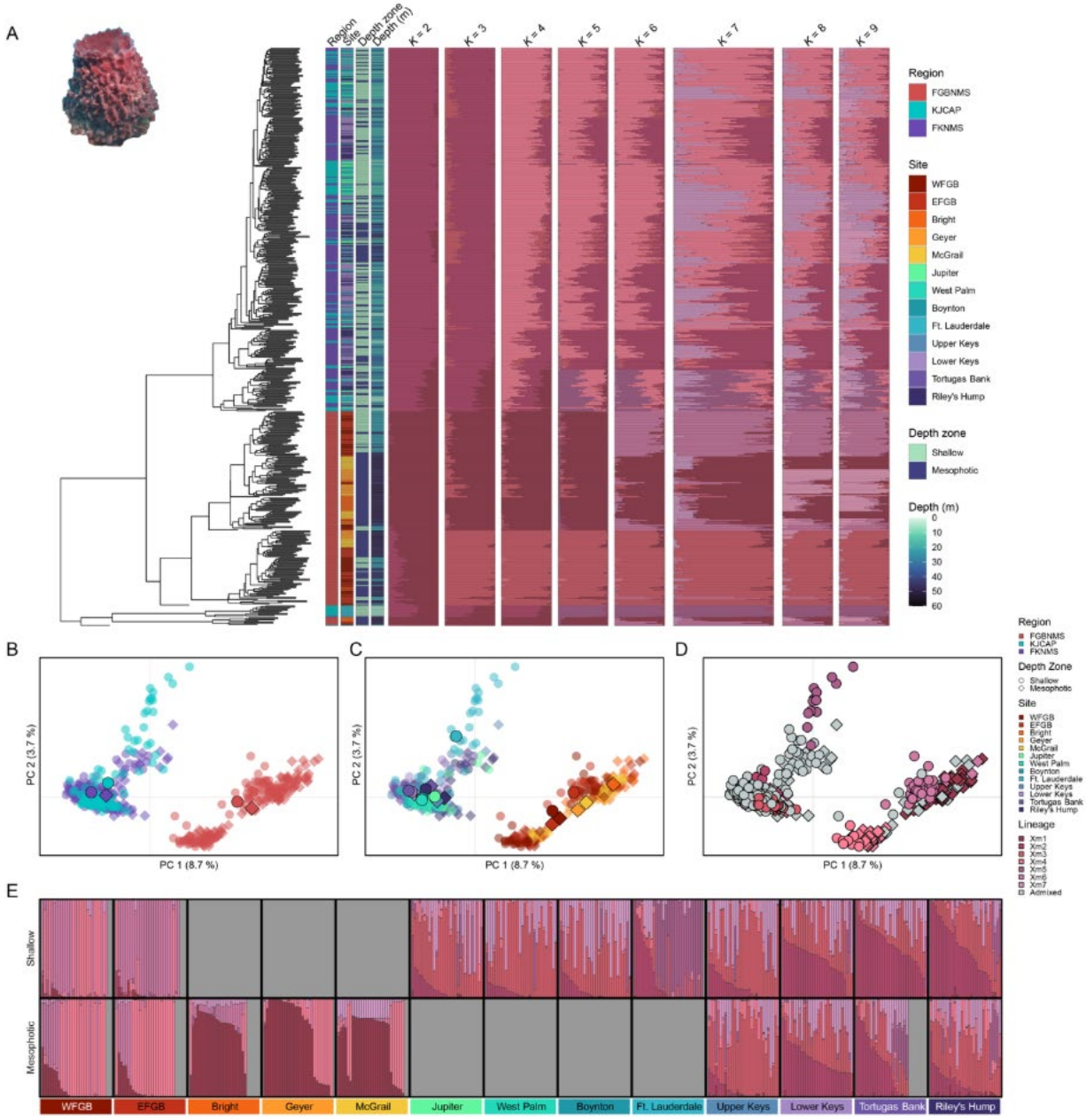

Figure 13. *Xestospongia muta* population genetic structure. A Dendrogram of samples based on IBS matrix from ANGSD with matching region, site, depth zone, and depth (m) data and structure plots for K =2–9 for each *X. muta* sample. **B** Principal component analysis from PCANGSD, where color represents sampling region and shape represents sampling depth zone. Larger, opaque shapes are sample population centroids and smaller, transparent shapes individual samples. **C** Same plot as **B** and with samples colored by sampling site. **D** Same plot as **B** and **C** with samples colored by lineage assignment from K = 7 data set. **E** Structure plot from NGSADMIX analysis with samples grouped by site and depth zone. Each bar represents an individual sample and the proportion of each color is the probability of membership to that genetic lineage.

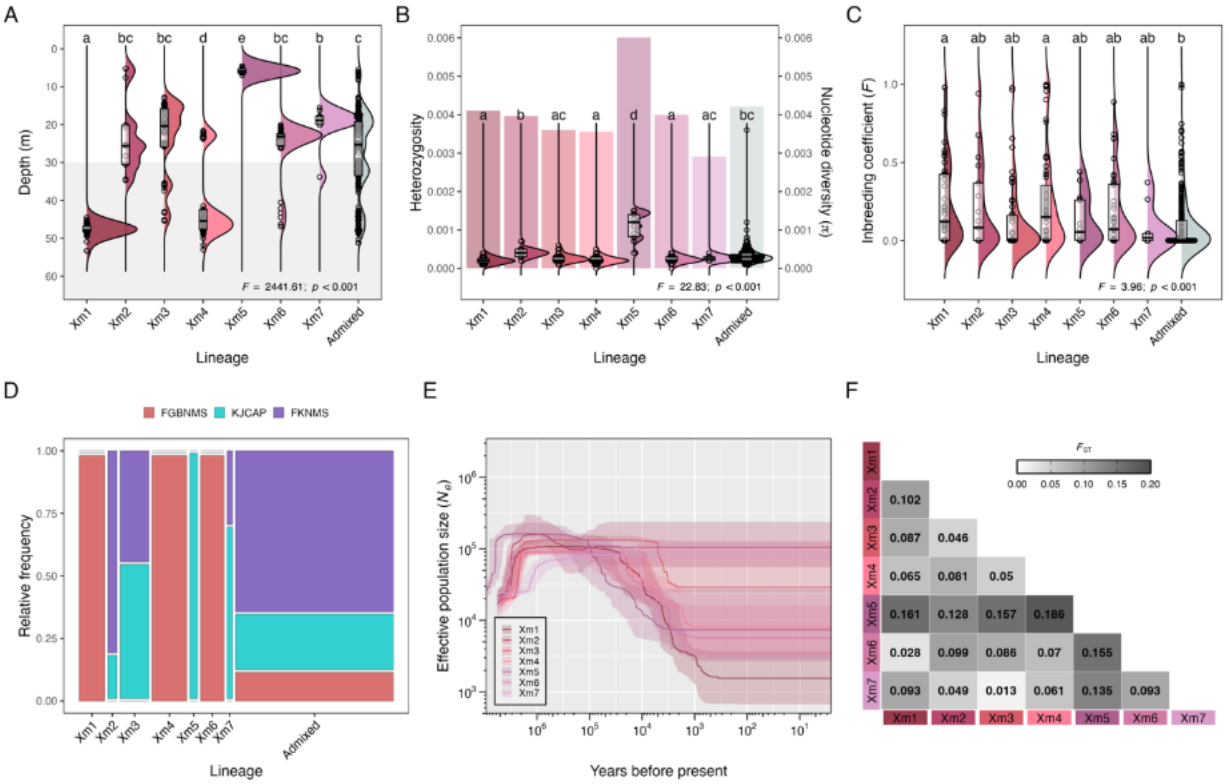

Figure 14. *Xestospongia muta* diversity and demographics. A *X. muta* lineage depth distribution. Shaded portion of graph indicates mesophotic depths. **B** Lineage heterozygosity across variant and invariant loci. Transparent bars behind violins represent nucleotide diversity (π) for each lineage. **C** Mean inbreeding coefficient by lineage. Letters indicate significant differences among lineages and Welch's ANOVA results are listed in **A**, **B**, & **C**. **D** Distribution of lineages across regions. Color of bars corresponds to sampling region. Width of bars is indicative of the relative proportion of samples assigned to that lineage. **E** Lineage effective population size through time. X-axis is thousands of years ago (KYA). Bounding ribbons are 75% confidence intervals. Note log scale for axes. **F** Pairwise fixation index (F_{ST}) heatmap among lineages. Darker coloration indicates higher F_{ST}.

4.3. Coral Salinity Threshold Experiments

The acute, chronic, and chronic+wounding studies are recapped briefly below, however, the bulk of effort in this period of performance was focused on 1) revisions to statistical analyses and data interpretation, and 2) qualitative comparisons between these results (Table 4).

Table 4. Table displaying acute hyposaline stress responses of corals found in the literature.

Species	Salinity (PSU)	Endpoint	Source
Porites astreoides	19	Mortality	This study
	25	Reduced polyp activity and bleaching, eventual mortality	
Montastraea cavernosa	19	Mortality	This study
	25	Reduced polyp activity and bleaching	
Siderastrea siderea	10	Decreased F_v/F_m	Chartrand et al. 2009
	Δ10	Reduced respiration and photosynthesis	Muthiga and Szmant 1987
Pocillopora damicornis	15	Bleaching and eventual mortality	Kongjandtre et al. 2021
	25	Bleaching	
Montipora capitata	20	Decreased time to onset of *Vibrio coralliilyticus* infection	Shore-Maggio et al. 2018
Acropora cytherea	26.6	50% reduction of fertility	Hedouin et al. 2015
	<26	50% mortality of larvae	
Acropora pulchra	27.5	50% reduction of fertility	Hedouin et al. 2015
	<26	50% mortality of larvae	

Acute Hyposalinity Stress

Acute hyposalinity at 19 PSU caused both *M. cavernosa* and *P. astreoides* fragments to exhibit rapid complete fragment mortality exceeding 50% (Figure 15), proving evidence that acute low salinity (e.g. <20 PSU) is more devastating than chronic exposure to intermediate hyposaline conditions (e.g. 25 PSU) for *M. cavernosa* and *P. astreoides* in Southeast Florida.

Hyposalinity events can pose significant risks to coral survival in regions heavily influenced by freshwater discharge. At St. Lucie Reef, one of the northernmost coral reefs in Florida, the lowest recorded salinity between 2015 and 2016 was 18 PSU (Shatters 2017; Studivan et al. 2021, Whitall et al. 2019), suggesting corals in this area may have been negatively impacted by hyposalinity. Both *M. cavernosa* and *P. astreoides* are less tolerant to acute hyposalinity than prominent backreef corals in the Caribbean and South Florida,

Siderastrea spp., which can tolerate salinities as low as 10–15 PSU (Muthiga & Szmant 1987; Chartrand et al. 2009). However, there are differential hyposalinity tolerances associated with coral life stages (Hédouin et al. 2015), and future larval studies of study species *M. cavernosa* and *P. astreoides* may yield further important data regarding the ecological impacts of late-summer freshwater events.

Chronic Hyposalinity Stress

While both species had a similar response to acute hyposalinity exposure, these two species showed differential responses to chronic exposure at 25 PSU, with *M. cavernosa* being more tolerant to extended moderate hyposalinity than *P. astreoides*. The results of this study were confirmed by an additional trial with similar conditions, which yielded extremely similar results and thus is largely not reported here. Mortality of 50% occurred for *P. astreoides* by day 18, yet *M. cavernosa* had only 10% overall mortality by day 21 (Figure 15).

Chronic Hyposalinity + Wound Stress

We found that M. cavernosa colonies exposed to this same intermediately stressful salinity survived more than 45 days in the chronic hyposlinity + wound experiment (Figure 15). This study provided strong evidence that while this coral is clearly resilient to extended periods of low salinity, it is less capable of combating additional stressors under these conditions.

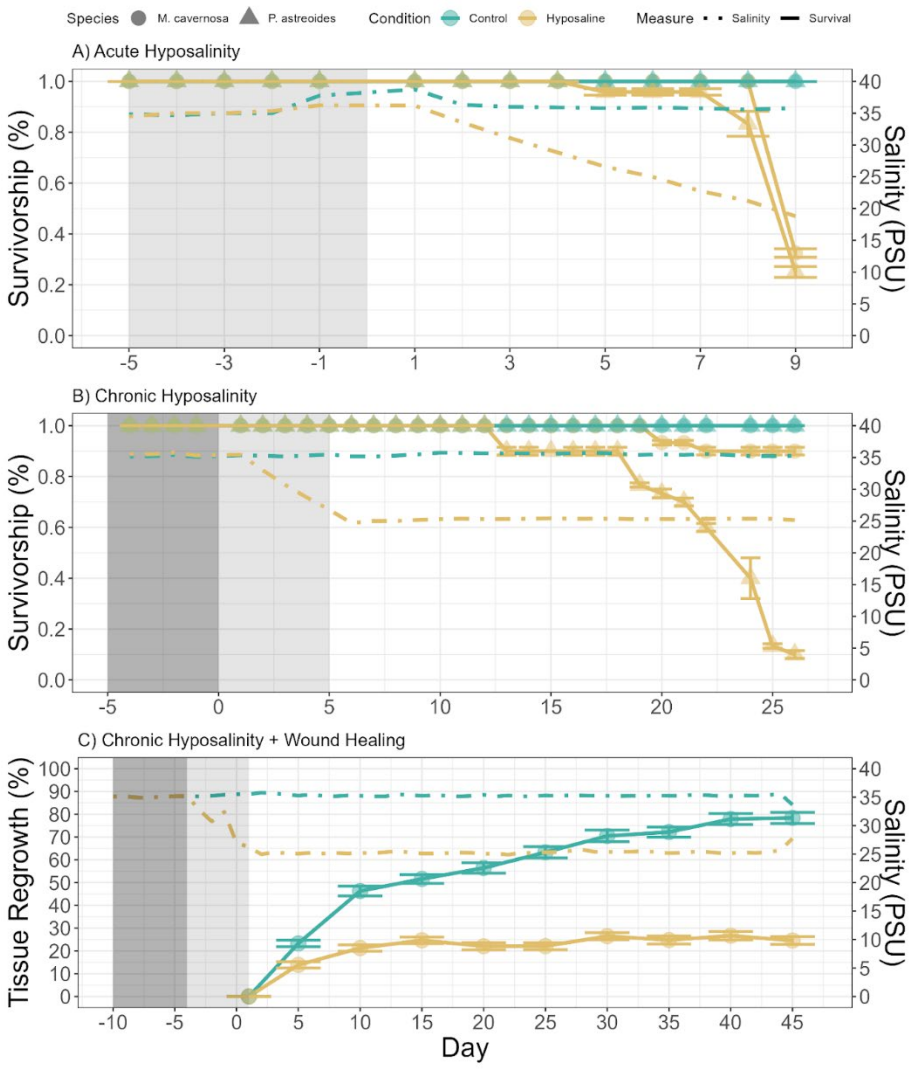

Figure 15. Mortality data for each experiment where salinity can be seen decreasing over time for treatment conditions (tan dashed) and holding steady in controls (teal dashed). In coordination, survivorship decreases for both *M. cavernosa* (circles) and *P. astreoides* (triangles) over time. The grey boxes represent the acclimation period preceding experimentation.

While polyp activity was reduced in hyposaline conditions across all three experiments, coloration impacts observed in the acute and chronic trials were absent in the chronic-wounding experiment (Figure 16), suggesting that interesting wounded corals may have been less likely to exhibit signs of bleaching.

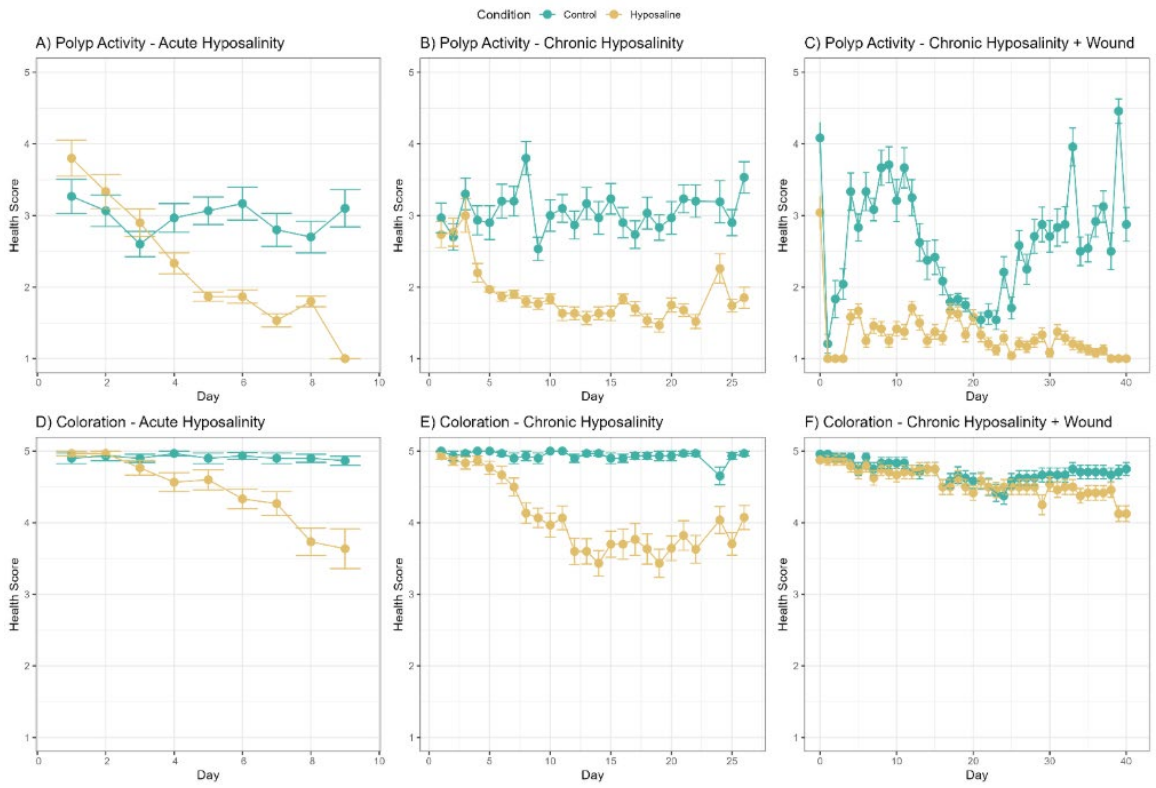

Figure 16. *Montastraea cavernosa* polyp activity and coloration scores throughout each experiment where points represent averages, bars represent standard error, and color denotes control (teal) vs treatment (tan). Each column represents a single experiment, and each row represents a different parameter. While polyp activity has more variation than coloration, over the course of each trial, scores for both parameters declined in the treatment condition. Error bars represent 95% confidence intervals.

4.4. Expanding Coral Restoration Efforts on St. Lucie Reef

After two years in February 2026, 81.25% of transplants survived. After the last monitoring interval for this fiscal year at 27 months, one additional colony died which brings the overall survival to 79.7%. Transplant survival has decreased approximately 10% each year over the last two years. When looking at only the large size class of the three species, 100% of large *Stephanocoenia intersepta* and *Siderastrea siderea* colonies are alive after 27 months, while 88.9% of large *Montastraea cavernosa* colonies remain alive (Fig. 17). Within the small size class 90% of *M. cavernosa*, 54.5% of *S. intersepta*, and 58.3% of *S. siderea* colonies were alive after 27 months (Fig. B). At this site, it is difficult to determine whether a colony is missing or is dead and covered in sediment or algae. Because of this, missing and dead have been combined into one category for these analyses. No significant difference in survival probability was found among species (Log-rank: $X^2 = 2.3$, $p = 0.3$), however there was a significant difference in survival probability between size classes (Log-rank: $X^2 = 43.1$, $p < 0.0001$). After 27 months, large colonies of *S. intersepta* and *S.*

siderea had a significantly greater survival probability than small colonies, while there was no difference between size classes of *M. cavernosa* (Figure 18).

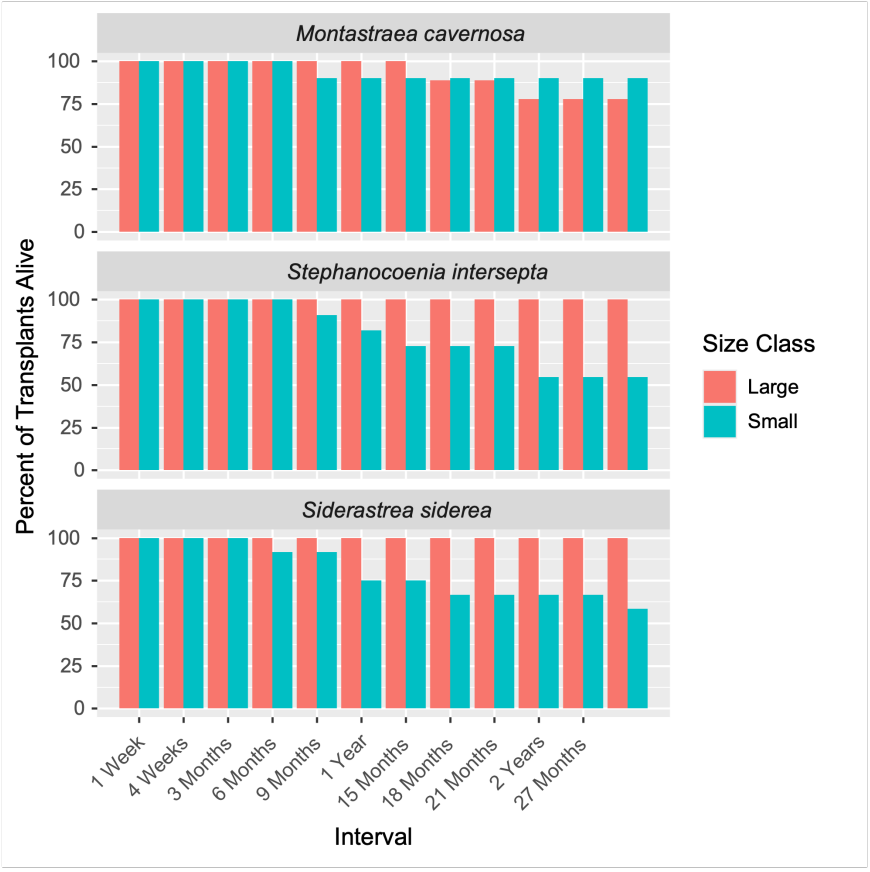

Figure 17. Total percent of transplanted colonies of the three species noted as alive during all monitoring intervals to date and separated into small (blue colored bars) and large (pink colored bars) size classes.

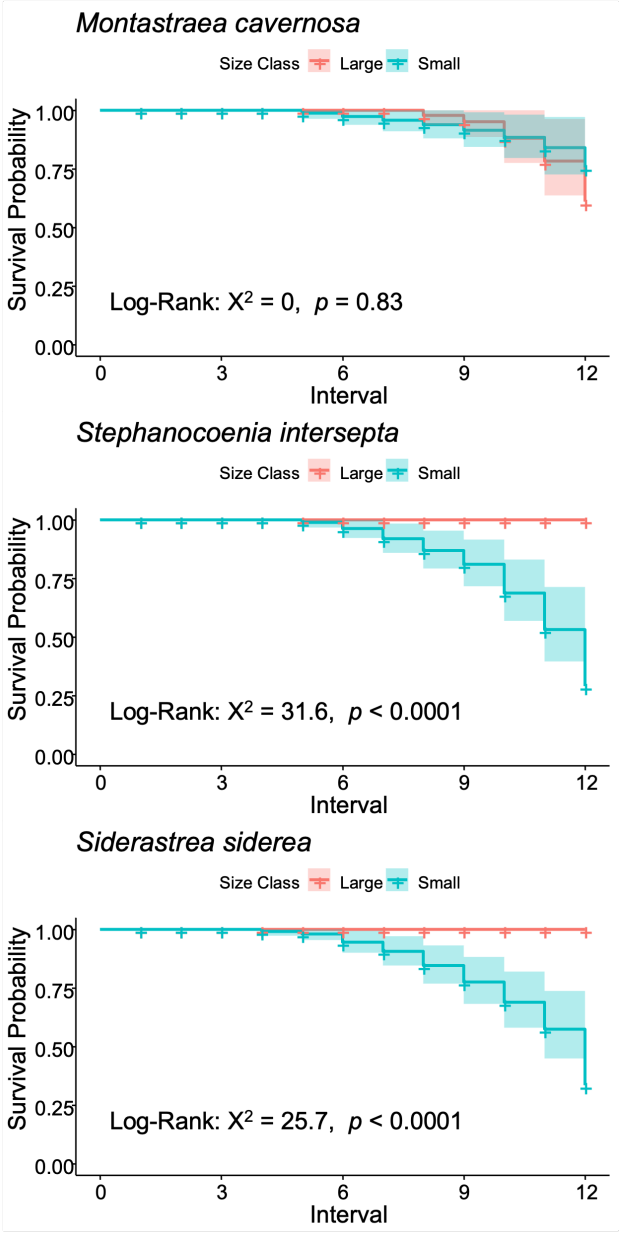

Figure 18. Kaplan-Meier survival curves show the survival probabilities between size classes for each species over all quarterly monitoring intervals from initial transplanting to the 27-month interval in May 2026 (Interval 12). Shaded regions surrounding each curve represent 95% confidence intervals. Test statistics from log-rank tests comparing differences in survival curves between size classes of each species are included, and *p*-values less than 0.05 indicate significant differences in survival probability.

In addition to overall survival, we also assessed yearly changes in live tissue surface area of the outplanted colonies over the first year using the scaled photos taken during monitoring. Included here are comparisons of growth after one and two years. Expanded analyses including all monitoring intervals are underway and will be included in the project manuscript for peer-review. As stated in last year's report, changes in average surface area and percent change in surface area among species or between size classes after 1 year were

insignificant. After two years, there is no significant difference in average surface area change between species (Mixed ANOVA: $F = 2.327$, $p = 0.110$) or size classes (Mixed ANOVA: $F = 2.097$, $p = 0.155$), yet there was a significant difference in the interaction between the two factors (Mixed ANOVA: $F = 4.681$, $p = 0.014$). Post-hoc pairwise t-tests with Bonferroni correction revealed there was a slightly significant difference in percent change in surface area between size classes but only for S. intersepta colonies (Pairwise T-test: $p = 0.0481$). While small colonies experienced a percent increase in average surface area ($14.926 \pm 49.791\%$) after two years and large colonies experienced an average percent decrease in surface area ($-2.268 \pm 32.267\%$), this difference is insignificant (Fig. 19).

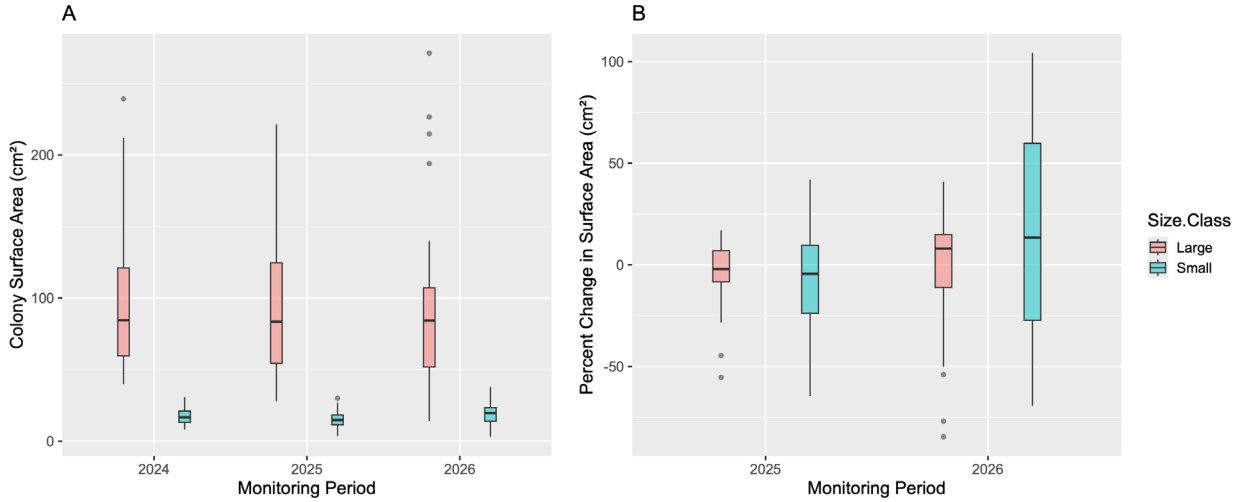

Figure 19. Box plots show the colony surface area at initial transplanting, one year, and two years (A); and percent change in surface area (B) between initial colony size and size at one and two years for each size class. All species are combined because there was no significant difference between them. Small size class is represented in blue, and the large size class is represented in pink.

4.5. Restoration Team Trials Algal Symbiont Analyses

We found that *Pseudodiploria clivosa* widely maintained *Breviolum* across both time points (Figure 20), whereas both *Montastraea cavernosa* (Figure 21) and *Orbicella faveolata* (Figure 22) exhibited stark shifts to the thermotolerant *Durusdinium* following the 2023 bleaching event. Furthermore, a clear spatial trend was observed in both *Orbicella* and *Montastraea*, with *Durusdinium* increasingly dominating the symbiont community in more southern restoration regions, from Miami-Dade through the Florida Keys.

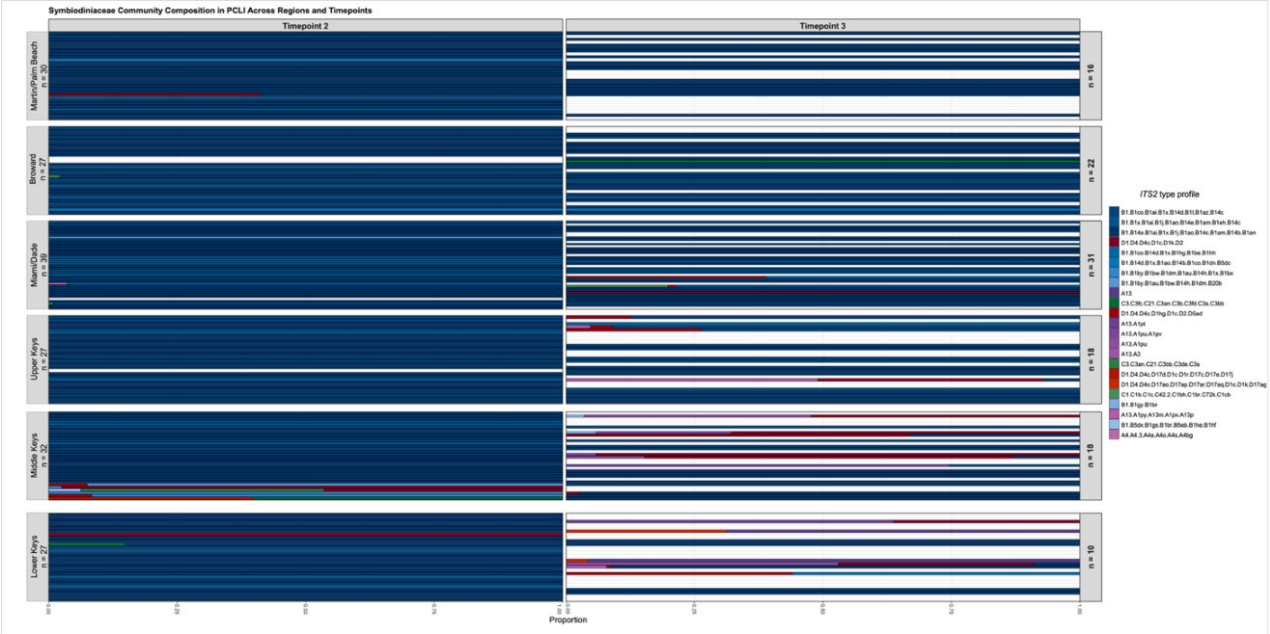

Figure 20. Bar plot visualizing ITS2 type proportions within each *P. clivosa* sample (n = 295) per region and time point. Bars are aligned for direct comparison of samples between time points. Blank spaces in either time point indicate the sample was not collected, either due to death or insufficient living tissue.

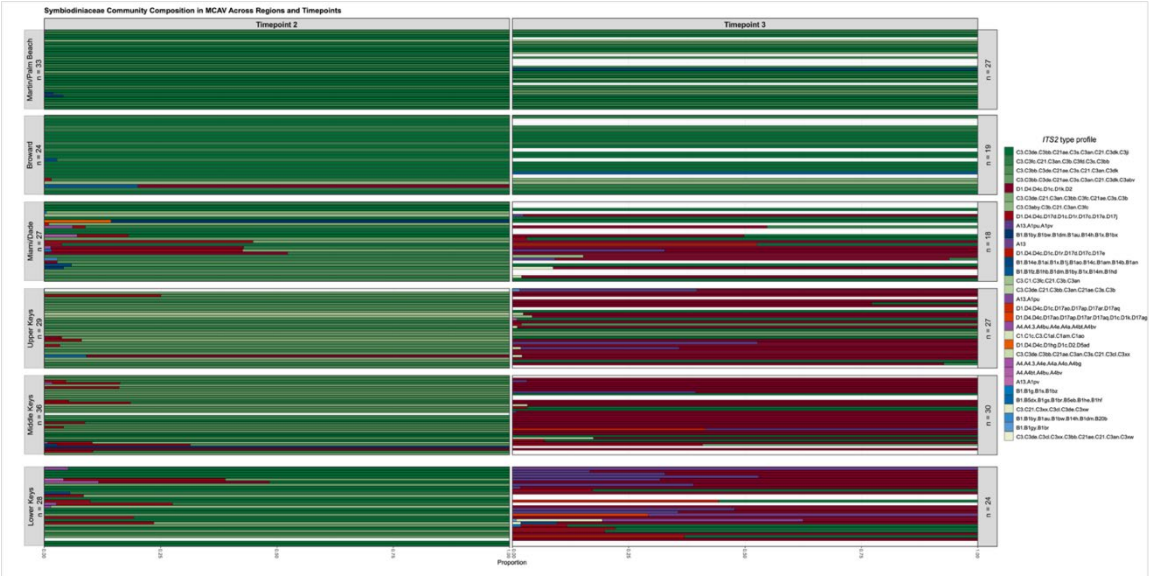

Figure 21. Stacked bar plot visualizing ITS2 type proportions within each *M. cavernosa* sample (n = 321) per region and time point. Bars are aligned for direct comparison of samples between time points. Blank spaces in either time point indicate the sample was not collected, either due to death or insufficient living tissue.

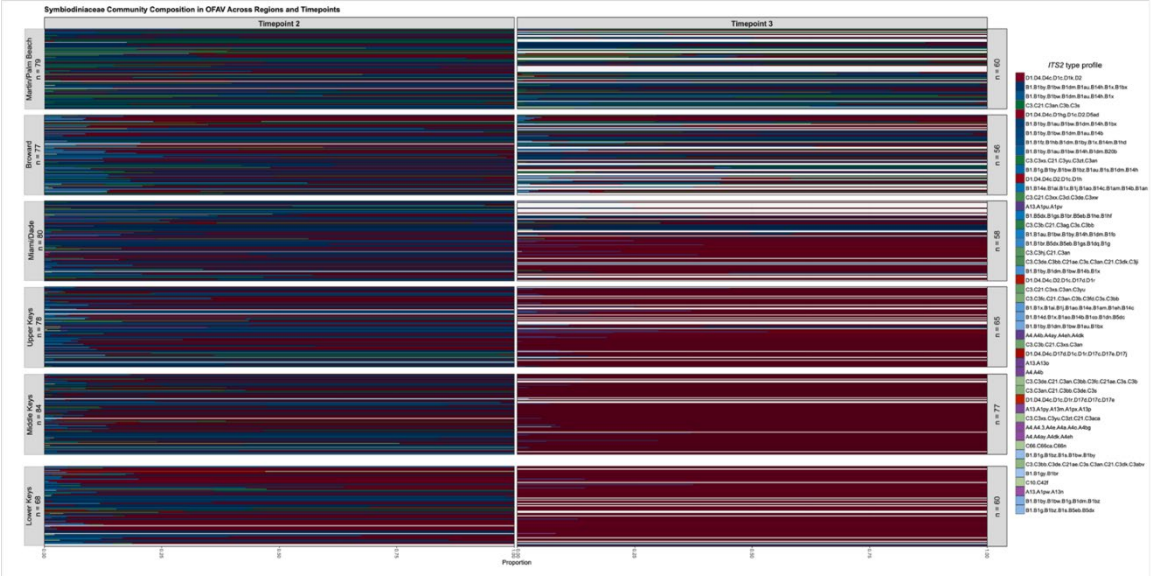

Figure 22. Stacked bar plot visualizing ITS2 type proportions within each *O. faveolata* sample (n = 839) per region and time point. Bars are aligned for direct comparison of samples between time points. Blank spaces in either time point indicate the sample was not collected, either due to death or insufficient living tissue.

SIMPER and pairwise comparisons across the expansive latitudinal gradient identified a stark geographic divide in community trajectories following the 2023 heatwave. Across all species pooled, *Durusdinium* was the primary driver of temporal dissimilarity between pre-stress (T2) and post-stress (T3) timepoints, accounting for 39% of the total dissimilarity (p = 0.001), followed by a substantial decline in *Breviolum* (30% dissimilarity contribution, p = 0.001). Regional pairwise SIMPER contrasts showed that baseline differences involving northern regions (Martin/Palm Beach vs. Broward and the Upper Keys) were initially explained by variations in *Cladocopium*. However, in comparisons involving more southern regions (Martin/Palm Beach vs. the Middle and Lower Keys), *Durusdinium* consistently emerged as the primary contributor to regional dissimilarity. This geographic shift coincided with an overall drop in total outplant survivorship from 73.1% at T2 (Sharp et al. 2024) down to 57.1% by T3.

At the individual host species level, clear variations in Symbiodiniaceae community plasticity emerged:

Pseudodiploria clivosa: Genus-level PERMANOVA revealed a highly significant Region x Timepoint interaction (F = 4.21, R^2 = 0.063, p = 0.0001). Despite significant temporal shifts localized within the Upper (p = 0.05) and Lower Keys (p = 0.006), population-level profiles remained overwhelmingly dominated by *Breviolum* across all regions (Figure 23). A significant temporal increase in *Durusdinium* was restricted to the Lower Keys (Wilcoxon, $p < 0.05$), while a localized upward trend in *Symbiodinium* was noted in the

Middle and Lower Keys (Wilcoxon, $p = 0.059$). Total survivorship for *P. clivosa* dropped severely from 65.2% to 41.5% post-heatwave.

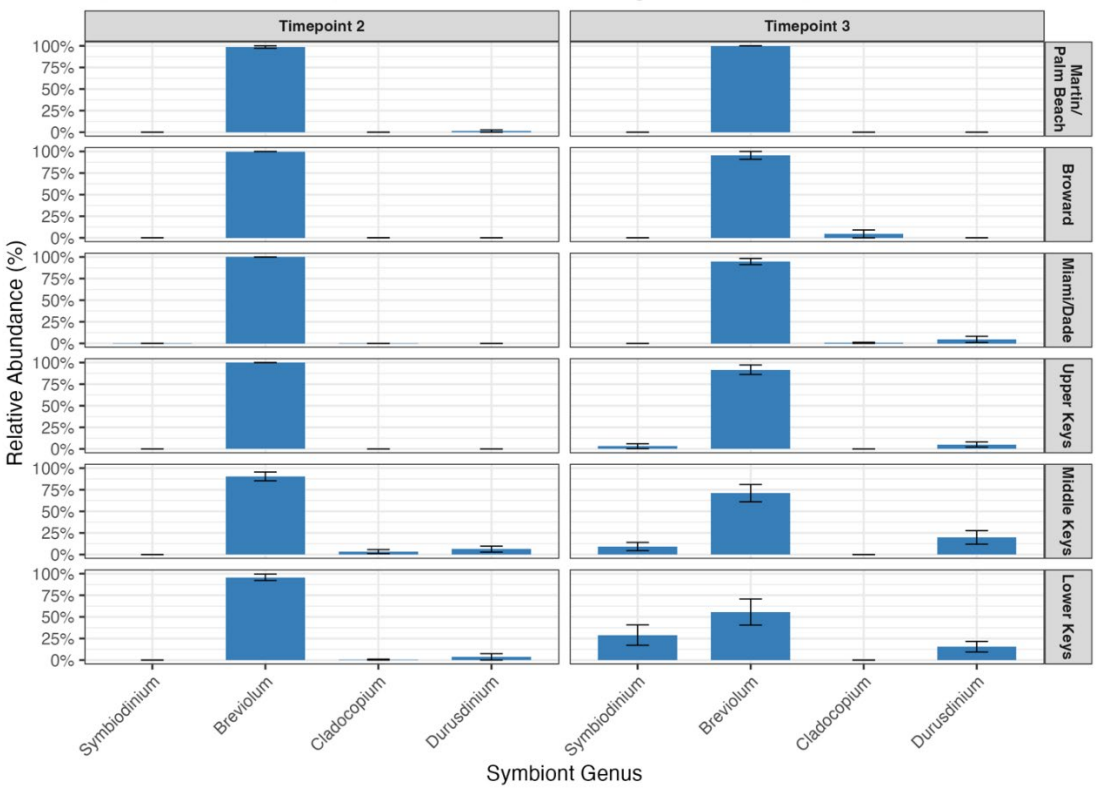

Figure 23. Relative abundances of Symbiodiniaceae genera within *Pseudodiploria clivosa* colonies across outplant regions and timepoints. Bars represent genus-level Symbiodiniaceae community composition within colony populations

Montastraea cavernosa: A strong Region x Timepoint interaction was likewise confirmed (all $p = 0.0001$), and post-hoc pairwise tests revealed that while northern regions (Martin/Palm Beach and Broward) remained compositionally stable, Symbiodiniaceae communities in southern outplants (Miami-Dade through the Lower Keys) shifted significantly between T2 and T3 ($p < 0.001$). This shift was defined by a severe decline in baseline *Cladocopium* and a concomitant increase in *Durusdinium* across all southern regions, alongside a significant expansion of *Symbiodinium* restricted to the Lower Keys (Wilcoxon, all $p < 0.05$; Fig. 2). Post-heatwave survivorship was 67.3%.

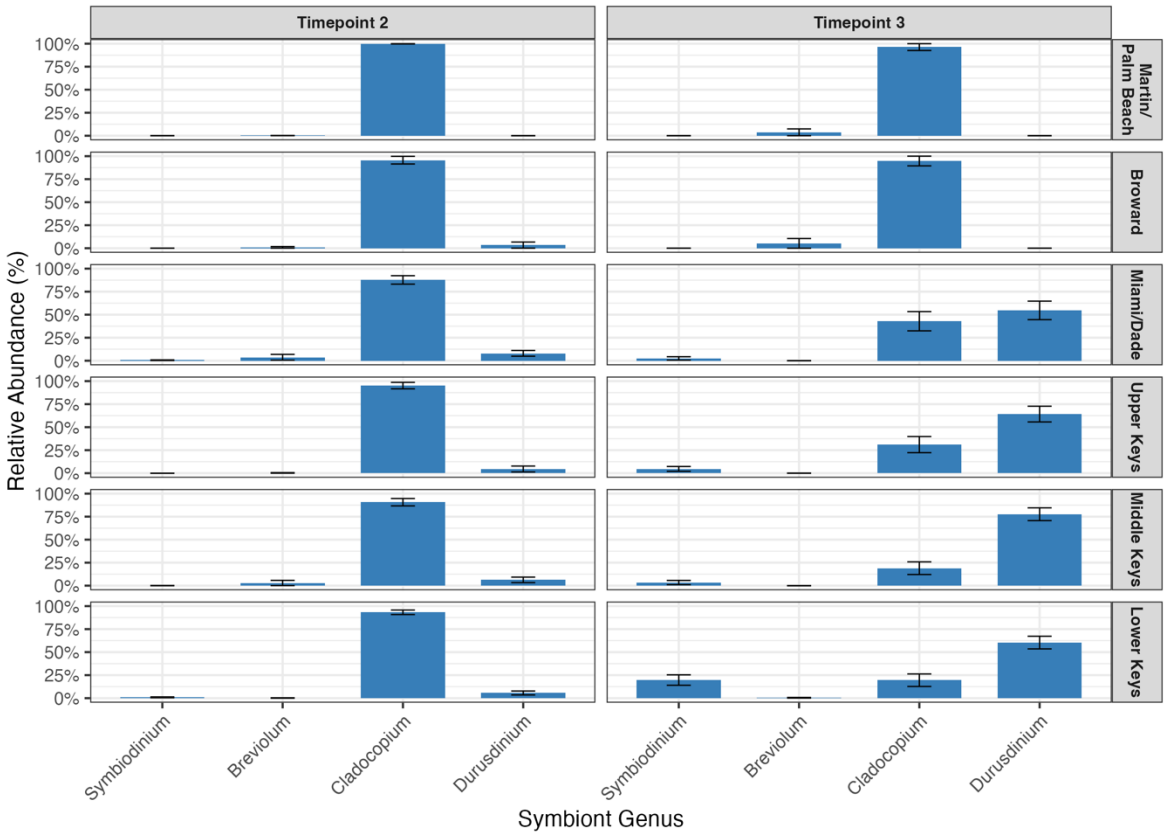

Figure 24 Relative abundances of Symbiodiniaceae genera within *Montastraea cavernosa* colonies across outplant regions and timepoints. Bars represent genus-level algal symbiont community composition within colony populations

Orbicella faveolata: Significant Symbiodiniaceae community changes were confirmed across all factors (all $p = 0.0001$). Mirroring *M. cavernosa*, post-hoc pairwise PERMANOVA indicated that significant temporal restructuring was isolated entirely within Miami-Dade throughout the Lower Keys ($p < 0.001$), while northern regions remained comparatively stable. At T2, colonies possessed mixed baseline assemblages of *Breviolum* and *Durusdinium*. By T3, *Breviolum* and *Cladocopium* decreased significantly in the south, while *Durusdinium* became wholly dominant throughout the Florida Keys (Figure 25). Low-abundance but statistically significant winter increases in *Symbiodinium* were detected in the Upper and Middle Keys (Wilcoxon, $p < 0.05$). Post-heatwave survivorship was 60.7%.

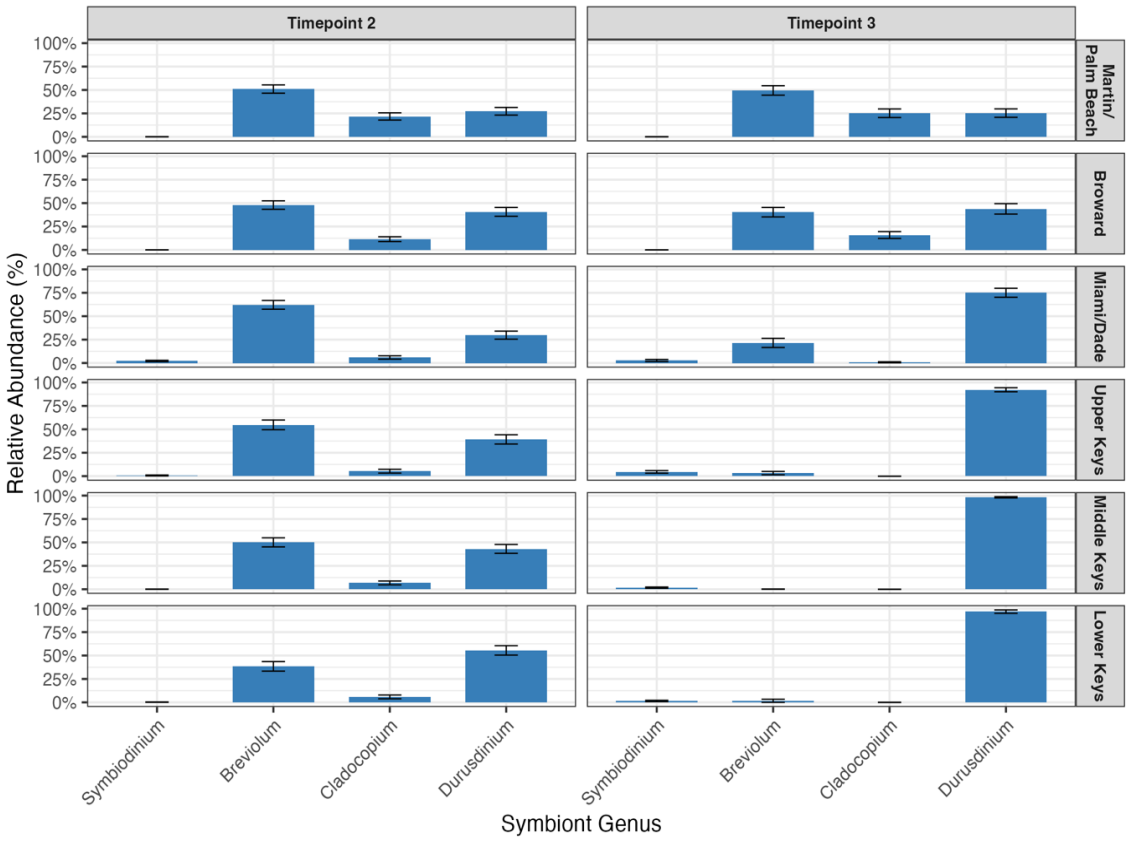

Figure 25. Relative abundances of Symbiodiniaceae genera within *Orbicella faveolata* colonies across outplant regions and timepoints. Bars represent genus-level algal symbiont community composition within colony populations

4.6. Thermal Stress and Disease

Overall, *M. cavernosa* experienced a 30% decline in photosynthetic efficiency (or effective dose, ED30), at 3.86 experimental degree heating weeks (eDHW) under acute stress and 4.79 eDHW under chronic stress. There were significant differences in ED30 values across genotypes. The overall mean ED30 across both acute and chronic trials was 4.31 eDHW, ranging from 2.96 to 6.61 eDHW. Trial (acute vs. chronic) and the interaction between colony and trial significantly impacted ED30 (trial: χ^2 (1) = 10.14, $p < 0.01$; interaction: χ^2 (11) = 25.10, $p < 0.01$), but not colony alone (χ^2 (1) = 14.94, $p = 0.19$). ED30 values were significantly different across trials (χ^2 (1) = 4.66, $p = 0.03$) when comparing trial alone, with an acute ED30 of 3.86 eDHW and a chronic ED30 of 4.78 eDHW (Figure 26). ED50 values were significantly different according to trial (χ^2 (1) = 17.54, $p < 0.01$), with an acute ED50 of 4.31 and a chronic ED50 of 6.33. $\Delta F_v/F_m$ was not significantly different in acute and chronic trials (χ^2 (1) = 0.01, $p = 0.90$). Decline width was significantly different according to trial (χ^2 (1) = 14.80, $p < 0.01$), averaging 2.68 eDHW under acute thermal stress and 9.79 eDHW under chronic thermal stress.

Figure 26: Combined results of acute and chronic thermal stress trials. (A) Weibull 1.3 thermal performance curves in experimental degree heating weeks. Horizontal dashed lines denote thermal thresholds, both ED30 and ED50. Bolded line indicates all genotypes pooled together, while shaded area indicates 95% confidence intervals. Faint lines indicate thermal performance curves for each genotype. ED30 occurred at an average of 4.30 eDHW and ED50 occurred at an average of 5.27 eDHW. (B) Boxplot of ED30 values across all genotypes according to trial. (C) Decline Width (eDHW) according to treatment. Decline width is calculated as ED95 – ED5.

Again, SCTLD disease transmission was unsuccessful, therefore further results are not presented here. This suggests either non-infectious etiologies that visually appear as SCTLD in the field or that the colonies used in this experiment were resistant.

5. PRELIMINARY CONCLUSIONS

For June 2025 to May 2026 stony coral tissue loss disease (SCTLD) prevalence remained low in Martin, Palm Beach, and Broward counties. At this point SCTLD is firmly endemic in the region, with low incidence of tissue loss lesions overall. Indeed our team and others have struggled to locate SCTLD positive colonies in the region for ex situ disease transmission experiments. Rather than improving environmental conditions, we hypothesize that loss of susceptible species is driving this trend. Fortunately, corals in the majority of KJCAP areas have displayed very little bleaching during this project period, indicating that St. Lucie Reef, Jupiter, Palm Beach, and to a lesser extent Ft. Lauderdale were fortunately spared bleaching events over the past 3 years as compared to reefs in the Florida Keys.

Through more than a decade of systematic population genetics efforts throughout the Gulf of America (Mexico) and Florida, we have discovered several cryptic lineages of *Montastraea cavernosa*, *Stephanocoenia intersepta,* and *Xestospongia muta* throughout Florida. Generally, shallow and mesophotic *M. caverosa* populations demonstrated higher connectivity to distant populations within the same depth zone than to adjacent populations across depth zones. However, exceptions to this pattern include the Northwest Gulf and the Florida Keys which exhibited relatively high vertical genetic connectivity. Furthermore, estimates of recent gene flow emphasize that mesophotic *M. cavernosa* populations are not significant sources for their local shallow counterparts, except for the Northwest Gulf populations.

Throughout the FGBNMS and Florida, *S. intersepta* is likely comprised of four cryptic lineages, while *X. muta* is most likely comprised of seven. In both species, there is a strong separation of between FGBNMS and Florida populations, with some level of overlap in the distribution of lineages across FKNMS and KJCAP in Florida. Genetic connectivity between FGBNMS and Florida MPAs appears to be negligible for both species, with no evidence of recent migration or shared lineages. Restoration planning can be improved by identifying and planning for this cryptic lineage diversity. Genetic diversity was higher in Florida as compared to Flower Garden Banks for these taxa, highlighting the importance of species- and region-specific assessments of population connectivity for conservation and restoration planning.

Our hyposalinity impacts study demonstrated that both *M. cavernosa* and *P. astreoides* from KJCAP were negatively affected by decreased salinity. While both species had a similar response to acute exposure, these two species showed differential responses to chronic exposure at 25 PSU, with *M. cavernosa* being more tolerant to extended moderate hyposalinity than *P. astreoides*. Colinies of *P. astreoides* experienced >50% mortality between 17 and 18 days, while *M. cavernosa* colonies had less than 20% mortality for at least 21 days. We were unable to determine if hyposalinity stress impacts disease susceptibility, however we did see slightly earlier mortality in *P. astreoides* colonies when both stressors were combined, than observed with chronic hyposaline stress alone.

Expanding coral restoration at St. Lucie Reef with transplants from Osborne tire reef has been largely successful with >80% survival after two years. For *S. intersepta* and *Siderastrea siderea*, larger transplant colonies demonstrated significantly greater survival probability than smaller colonies. However, fragment size had no impact on the highly successful *M. cavernosa* transplants. This study provides evidence for the efficacy of transplanting corals across regions within KJCAP, at least in terms of multiyear survivorship. Other potential tradeoffs including reproductive capacity, potential disease

transmission, or impacts on population genetics and diversity, should also be considered in restoration planning efforts.

Through our collaborative efforts with the Restoration Research Consortium, we observed a stark latitudinal divergence in outplanted corals' algal endosymbiont communities following the 2023 bleaching event. Multivariate analyses confirmed that post-bleaching community trajectories were strongly shaped by regional thermal regimes. In the cooler, northern regions (Martin County to Broward), Symbiodiniaceae communities remained stable, and outplant survival was higher. Conversely, outplants in southern regions (Miami-Dade through the Lower Keys) experienced the earlier and more prolonged thermal stress that drive extensive algal endosymbiont community restructuring. This stark spatial divide across an extensive geographic range highlights how localized climate anomalies dictate the real-time success of restoration efforts, driving patterns consistent with the adaptive bleaching hypothesis. The shifts toward *Durusdinium* within corals in the southern areas may have contributed to their short-term survival during the extreme 2023 bleaching event.

Finally, we found that acute and chronic stress treatments yielded significantly different outcomes for *M. cavernosa* from KJCAP. These results suggests that *M. cavernosa* is more vulnerable to acute thermal stress and slightly more resilient to chronic thermal stress. Both types of stress are expected to increase under future ocean conditions, with more extreme fluctuations in temperature and shifts to warmer baseline temperatures. Experimental determined thresholds in *M. cavernosa* suggest colonies of this species in KJCAP will be able to withstand marginal increases in baseline temperature, but will be less resilient to increased temperature fluctuations. Acute thermal bleaching among *M. cavernosa* in KJCAP can be expected whenever conditions exceed 4 Degree Heating Weeks (DHW), similar to global averages reported for other coral species. These data allow better bleaching predictions in KJCAP based on thermal stress and accumulated DHW.

6. RECOMMENDATIONS

Recommendation 1: *Continue quarterly monitoring in Kristin Jacobs Coral Aquatic Preserve and St. Lucie Inlet Preserve State Park to capture trends in coral ecosystems, impacts of episodic events, and evidence of resilience/recovery.* More frequent monitoring efforts (e.g. quarterly) help us to better link events to impacts as compared to annual monitoring surveys. Having both will provide complementary data sets that best capture the changes and trends in the Southeast Florida region.

Recommendation 2: *Advance coral conservation initiatives with support from Magnuson-Stevens Act and implement actions/regulations for Kristin Jacobs Coral Aquatic Preserve.* Efforts to reduce stressors or known impacts to coral reef communities should be

implemented to enhance the likelihood of coral resilience and recovery, particularly with respect to water quality. Furthermore, efforts to develop more robust coral restoration programs should include research toward sexual propagation, ex situ and in situ nurseries, subsequent outplanting, and continued testing of outplant resilience to SCTLD.

Recommendation 3: *Advance coral population genetics to support effective management and restoration for coral populations and communities in Florida.* Additional effort and resources are needed to understand Florida's intraspecies genetic diversity. These assessments need sampling from the greatest number of locations and depths feasible. Expanding our efforts has led to the discovery of cryptic lineages within four coral species thus far, which impact our management and restoration strategies. Successful coral restoration approaches will require knowledge of genetic stocks among various coral populations to design and implement effective restoration plans across regions and depths.

Recommendation 4: *Update management criteria to keep salinities on coral reefs above 20 PSU for short term exposures (1-2 days), and above 25 PSU if freshwater releases will last longer than one week.* Currently corals' responses to freshwater releases and subsequent impacts on coastal nearshore salinities are currently not considered in management criteria. Our results suggest that when exposed to reduced salinity levels, corals are both more likely to perish and significantly impeded in their recovery from physical damage.

Recommendation 5: *Continue restoration efforts with hypothesis driven designs to continue improving and optimizing restoration success.* The RTT and Osborne transplant experiments demonstrated that outplants of SCTLD susceptible species can survive, grow, and fuse. However, significant differences have been observed among species, outplant regions, and coral sources. Further experiments to assess the impacts of these and other factors on outplant survivorship, growth, and reproduction need to be coupled to the genomic efforts discussed above.

Recommendation 6: *Consider thermal stress when implementing restoration strategies.* Experimentally derived thermal thresholds in *Montastraea cavernosa* provide evidence that outplant efforts should be avoided when conditions near or exceed 4 DHW.

7. LITERATURE CITED

Chartrand, K. M., Durako, M. J., & Blum, J. E. (2009). Effect of hyposalinity on the photophysiology of *Siderastrea radians*. *Marine Biology*, *156*(8), 1691–1702. https://doi.org/10.1007/s00227-009-1204-3

Eckert, R. J., Reaume, A. M., Sturm, A. B., Studivan, M. S., & Voss, J. D. (2020). Depth influences Symbiodiniaceae associations among *Montastraea cavernosa* corals on the Belize Barrier Reef. *Frontiers in Microbiology*, *11*, Article 518. doi.org

Hédouin, L., Pilon, R., & Puisay, A. (2015). Hyposalinity stress compromises the fertilization of gametes more than the survival of coral larvae. *Marine Environmental Research*, *104*, 1–9. https://doi.org/10.1016/j.marenvres.2014.12.001

Hume, B. C. C., Ziegler, M., Poulain, J., Pochon, X., Romac, S., Boissin, E., De Vargas, C., Planes, S., Wincker, P., & Voolstra, C. R. (2018). An improved primer set and amplification protocol with increased specificity and sensitivity targeting the *Symbiodinium* ITS2 region. *PeerJ*, *6*, Article e4816. doi.org

Klepac, C., Kenkel, C., Sproles, A., Beal, J., & Voss, J. (2015). Seasonal stability of coral-*Symbiodinium* associations in the subtropical coral habitat of St. Lucie Reef, Florida. *Marine Ecology Progress Series*, *532*, 115–122. doi.org

Klepac, C. N., Petrik, C. G., Karabelas, E., Owens, J., Hall, E. R., & Muller, E. M. (2024). Assessing acute thermal assays as a rapid screening tool for coral restoration. *Scientific Reports*, *14*(1), Article 1898. doi.org

Kongjandtre, N., Wattana, T., Veerapitipath, V., & Chinchana, A. (2021). Effect of hyposalinity on coral bleaching and survival in a hard (*Pocillopora damicornis*) and soft coral (*Sarcophyton* sp.). *Naresuan University Journal: Science and Technology*, *30*(2), 38–49. doi.org

Muthiga, N. A., & Szmant, A. M. (1987). The effects of salinity stress on the rates of aerobic respiration and photosynthesis in the hermatypic coral *Siderastrea siderea*. *The Biological Bulletin*, *173*(3), 539–551. https://doi.org/10.2307/1541699

Shatters, A. (2017). *Effects of St. Lucie estuarine discharge water and thermal stress on the coral Montastraea cavernosa* [Master's thesis, Florida Atlantic University]. FAU Digital Library.

Sharp, W., Muller, E. M., Bourque A., Giliam, D. S., Kemp, D. W., Lirman, D., Parsons, K. T., Shea, C. P., & Voss, J. D. (2024). *Large-scale outplanting designed to assess coral restoration feasibility in response to stony coral tissue loss disease* (Final Report). National Oceanic and Atmospheric Administration.

Shore-Maggio, A., Aeby, G. S., & Callahan, S. M. (2018). Influence of salinity and sedimentation on *Vibrio* infection of the Hawaiian coral *Montipora capitata*. *Diseases of Aquatic Organisms*, *128*(1), 63–71. doi.org

Studivan, M. S., Shatters, A., Dodge, D. L., Beal, J. L., & Voss, J. D. (2021). Synergistic effects of thermal stress and estuarine discharge on transcriptomic variation of *Montastraea cavernosa* corals in southeast Florida. *Frontiers in Marine Science*, *8*, Article 662220. https://doi.org/10.3389/fmars.2021.662220

Sturm, A. B., Eckert, R. J., Méndez, J. G., González-Díaz, P., & Voss, J. D. (2020). Population genetic structure of the great star coral, *Montastraea cavernosa*, across the Cuban archipelago with comparisons between microsatellite and SNP markers. *Scientific Reports*, *10*(1), Article 15432. doi.org

Whitall, D., Bricker, S., & Cox, D. (2019). *Southeast Florida Reef Tract water quality assessment* (NOAA Technical Memorandum NOS NCCOS 263). National Oceanic and Atmospheric Administration. https://doi.org/10.25923/KYFT-JA41